

Chapter 2

Fundamentals of Organic Lasers

Abstract In this chapter the main characteristics and specificities of organic solid-state lasers are presented. We particularly highlight these aspects which are important for organic lasers and specific to them, and which are therefore not usually treated in classical textbooks on lasers. The objective of this chapter is to present a quite general, while not exhaustive, overview of the photophysics of organic compounds that are directly useful to understand the physics of organic lasers, as well as a theoretical framework suited to the description of these lasers in most practical situations.

In this section we first present (Sect. 2.1) the basics of pi-conjugated systems: their general properties, and why they have semiconducting properties in neat solids. We then review (Sect. 2.2) their photophysical properties: how they absorb and emit light, and why they do this very well but only in the UV–visible range. Organic lasers have a distinctive dynamical behavior compared to other gain media, in particular they are not able to work (at least up to now) in the CW regime: this peculiarity is due to the existence of triplet states, which are examined with some detail in Sect. 2.3. As organic emitters are never alone in a solid-state medium but surrounded by other emitters, of the same kind or different, in the ground or in the excited state, many intermolecular or quenching effects may arise, which strongly affect the laser performance (FRET, exciton–exciton annihilation, exciton diffusion, etc.): they are discussed in Sect. 2.4. In Sect. 2.5 we examine how these photophysical properties affect the laser operation and in particular the rate equations. Then finally in Sect. 2.6 we gather the concepts presented during all the preceding sections to deal with organic lasers dynamics, establish a condition for CW lasing and discuss the limits on the pulsewidth from practical systems.

2.1 PI-Conjugated Molecular Systems

2.1.1 General Properties

Organic compounds consist mostly of carbon and hydrogen with a few heteroatoms such as oxygen, nitrogen or sulfur for instance. Due to the large number of binding configurations of carbon, organic materials form a huge assembly which represents several millions of reported different compounds. Not all of them, though, are suitable for lasing.

Carbon atoms have six electrons, with a ground state configuration $1s^2 2s^2 2p^2$, meaning that the s orbitals are fully occupied whereas two out of the three p_x , p_y and p_z orbitals are occupied by one electron each. When a carbon atom makes a bond with another atom, hybridization occurs between s and p orbitals. When the C atom connects via four single bonds to other atoms, sp^3 -hybridization occurs and the four outer electrons are arranged at the corners of a tetrahedron. These bonds are qualified as σ -bonds, as they exhibit a cylindrical symmetry. Such saturated compounds are good electrical insulators. Some examples are alkanes, or saturated polymers such as polyethylene ($-\text{CH}_2-\text{CH}_2-$)_n, polystyrene ($-\text{CH}_2-\text{CH}(\text{Ph})-$)_n or polypropylene ($-\text{CH}_2-\text{CH}(\text{CH}_3)-$)_n.

As far as optical and electrical properties are concerned, molecules containing double or triple bonds are more complex and more interesting. Let's consider the archetypical example of ethylene ($\text{CH}_2=\text{CH}_2$) represented in Fig. 2.1: in this simple case, carbon atoms exhibit sp^2 -hybridization. The three sp^2 hybrid orbitals are arranged in a trigonal planar geometry, pointing to the three corners of an equilateral triangle, with angles of 120° between them; the unhybridized $2p_z$ orbitals are perpendicular to this plane and overlap side-by-side to form a weaker π bond.

If the molecule presents an alternation of simple and double bonds over a planar segment, the system is said to be *pi-conjugated*. Such systems exist in many forms (small molecules, conjugated polymers, molecular crystals) that will be described in more detail in Chap. 3. The simplest examples of pi-conjugated molecules, useful for understanding the underlying physics although they are not directly useful for lasing, are benzene and butadiene (see Fig. 2.2). The overlap between the π orbitals in those structures allows for the *delocalization* of the electrons over the whole conjugated segment, meaning that the picture of the molecule as a single Lewis formula of localized single and double bonds is not valid any more. The orbitals lose their pure sp^2 -hybridized character, and the molecule is instead more conveniently described by a superposition of resonant mesomeric forms. The π electrons do not belong to a single bond or atom, but rather to a group of atoms. A naïve picture of delocalization consists in thinking of a *pi*-electron moving along the conjugated chain as a “flip-flop” between single and double bonds.

The alternation of double and single bonds is a necessary condition for pi-conjugation, but not sufficient, as the bonds should also lie in the same plane to enable electron delocalization. For instance, benzene, with its 6 carbon atoms

Fig. 2.1 Illustration of σ and π orbitals in ethylene

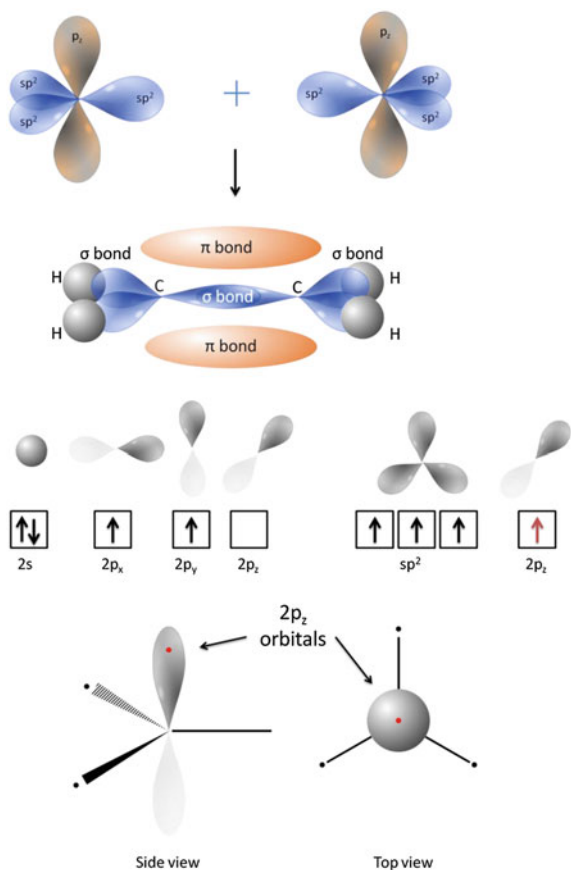
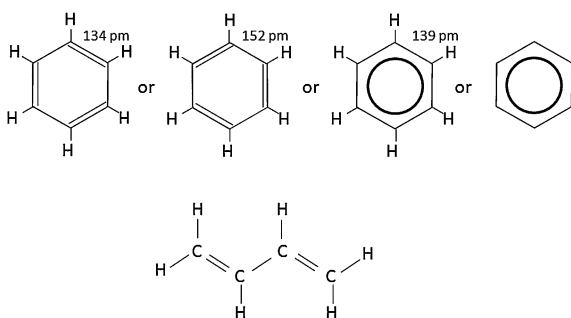


Fig. 2.2 Two simple and archetypical examples of pi-conjugated systems: benzene (*top*) and 1,3-butadiene (*bottom*). For both cases, classical Lewis formula are approximate and unsatisfactory pictures of reality, and the molecules are rather described by a superposition of different mesomeric forms



linked at the corners of a regular planar hexagon (see Fig. 2.2), is the archetype of aromatic conjugated systems. In contrast, cyclooctatetraene, which is a regular octagon with alternating simple and double bonds, adopts a “tub” nonplanar conformation and is therefore not aromatic (and only weakly conjugated). Most of

practical dyes only have a portion of the molecule that is conjugated, referred to as the active unit or the chromophore unit, the rest of the molecule being for instance a saturated alkyl chain added for solubilization (see MEH-PPV for example [1]) or bulky side groups added to prevent stacking of the pi-orbitals between them in adjacent molecules, like in dendrimers [2] or in small molecules with bulky side substituents [3].

When more and more p_z orbitals are shared to form a conjugated system, the energy between molecular orbitals decreases, in a similar way as energy states of a free electron in a box get closer when the box dimensions increase (see next subsection). In particular, the energy gap between the Highest Occupied Molecular Orbital (HOMO) and the Lowest Unoccupied Molecular Orbital (LUMO) which governs the optical properties, becomes smaller. The absorption band of conjugated systems then occurs at wavelengths above 200 nm, making such compounds suitable for optical excitation in the UV-visible part of the spectrum.

2.1.2 Organic Semiconductors

2.1.2.1 Charge Delocalization and Polaron States

The delocalization of electrons is also the key to understand the semiconducting properties of pi-conjugated systems, in a sense which however needs some clarification. The optical gap defined by $E_{\text{gap}} = E(\text{LUMO}) - E(\text{HOMO}) - E_b$ (where E_b is the binding energy of the exciton, defined in the following) varies in the range $\sim 1\text{--}4$ eV for pi-conjugated systems, which makes them fall into the category of insulators, the “conduction band” (LUMO) of the molecule being almost empty at room temperature. Stated otherwise, there are very few free carriers available (typically less than 10^{14} cm^{-3} in organic semiconductors, where the chromophore density is around 10^{21} cm^{-3}) [4].

Conjugated systems are semiconductors as far as we consider molecular solids (organic crystals, polymers, neat films of small molecules...) made of an assembly of molecules in contact with each other, either in an ordered or disordered medium. The term “contact” just means here that there is a possibility for a charge to travel from a molecule to another, a loose definition which excludes dye-doped nonconductive polymers or dye-doped glasses, and obviously dyes in liquid solutions or gas phase. In order to understand the semiconducting properties, we have to consider that among the molecular assembly we have a *doped* molecule, that is, with an additional or a missing electron on it. Indeed electrical conduction makes sense only whenever one of the bands is partially empty; here it translates in saying that the HOMO or the LUMO level contains only one electron instead of two. From a chemist’s point of view, these states are oxidized or reduced forms of the molecule, namely charged radical ions. From the physicist’s point of view, the same objects are often referred to as “holes” (when one electron is missing in the HOMO) or “electrons” (when one extra electron is added in the LUMO); however

the adequate word to describe these states is a *polaron*. First of all, as organic pi-conjugated molecules are rather big molecules (with molecular weights over a few hundreds for the simplest dyes) they have many vibrational modes and may be thought of as a complex system of springs coupled together in a very classical mechanics point of view. Adding or removing a charge on such a molecule may then not happen without a significant vibrational relaxation whose aim is to seek the new free energy minimum that will take into account the presence of the extra charge. Furthermore the nearby neutral molecules will react at the presence of a charge by a slight displacement of their inner charge clouds, creating a macroscopic electrical polarization around the doped molecule, which in turn will lead to a further stabilization of the latter. A *polaron* is the quasi-particle corresponding to the charged molecule and its accompanying polarization field; the electron polaron state has a lower energy than the genuine LUMO state (basically it means that more energy is required to pull the electron out of the molecule than it would be for an isolated molecule in gas phase), and symmetrically the hole polaron state lies higher in energy than the original HOMO (see Fig. 2.3), by an amount called

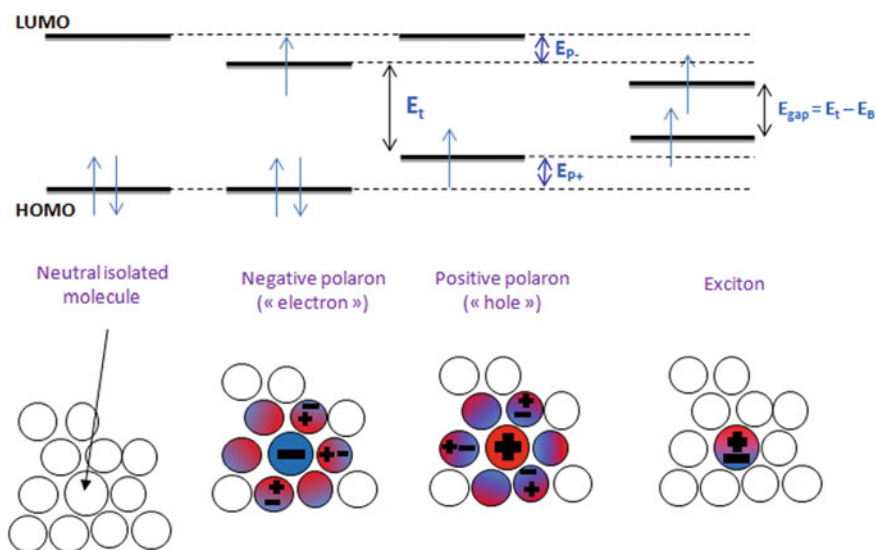


Fig. 2.3 Illustration of relevant energy levels in organic semiconductors. The HOMO and LUMO states pertain to isolated molecules, in gas phase or in a nonpolar solvent/nonpolar solid matrix. In neat solid materials where the molecules form organic semiconductors (OSC), the neighboring polarizable molecules create a charge cloud around the charge which modifies the energy levels of the molecular ion by an amount E_{p+} (for holes) and E_{p-} (for electrons): the whole entity is called a polaron. In an OSC the effective “transport gap” between electrons and holes is defined as $E_t = E(\text{LUMO}) - E(\text{HOMO}) - E_{p+} - E_{p-}$ [99]. The optical gap, usually measured at the onset of optical absorption, includes an exciton binding energy term E_B , because it requires some extra energy to separate a pair of coulombically-bound charges onto different molecules ($E_{gap} = E_t - E_B$)

the polaron binding energy, whose typical order of magnitude is a few tens of eV (0.137 eV calculated in anthracene [5] or 0.29 eV in TPD [6]).

This charge added on the molecule is also delocalized over the conjugation segment and can be thought of as a mobile charge. A mobile charge on a molecular moiety does not still make the medium a conductor, because in order to carry electrical current, charges must be able not only to travel within one molecule, but also to pass from a molecule to another and join electrodes. In a disordered medium (that is, most of practical polymers or small-molecular films used for organic optoelectronics applications) this is usually done by “hopping”, basically through tunneling, from a conjugated site to another, or in a more classical “bandlike” conduction picture in the case of organic crystals. The hopping mechanism is highly inefficient and clearly the limiting factor which explains the very low carrier mobilities in organic semiconductors compared to inorganic semiconducting crystals. Details about charge transport in OSCs can be found in Refs. [7–12].

2.1.2.2 Excitons

In addition of a difference in the nature of charge carriers, the nature of neutral excited states is also very different. These states are called *excitons* because they have the ability to diffuse from a site to another and hence comply with the definition of an exciton being a mobile excitation quasi-particle. The main difference between excitons in inorganic and organic semiconductors arises from the fact that in OSCs electrons are only weakly delocalized over a small length scale even in the case of molecular crystals or conjugated polymers. As a result they have two important peculiarities as compared to their inorganic counterparts.

1. The first one is a considerable binding energy, linked to the strong localization of excitons in a single molecular site (and accordingly to a small dielectric material constant $\epsilon_r \sim 3$ in OSCs versus ~ 13 for gallium arsenide, which means that there is no efficient screening of columbian interactions), defined as the energy required to break an exciton into a pair of uncorrelated electrons and holes:

$$E_b = \frac{e^2}{4\pi\epsilon_0\epsilon_r d_{e-h}}$$

where d_{e-h} is the separation distance of the charge carriers. The typical values are 0.5–1.5 eV for organic crystals [13] and usually less (0.2–0.5 eV) for conjugated polymers [14]. In OSCs where electrons and holes can hop from a site to another, this strong binding energy means that excitons are particularly stable against charge separation. The situation in terms of energy levels is summarized in Fig. 2.3.

2. The second difference is the existence of well-defined spin states (singlet and triplet) for excitons which makes them no different from isolated molecules in this respect. The triplet excited states have usually a lower energy level than the singlet excited state by an amount called the exchange energy ΔE_{ST} , which will be discussed in more details in [Sect. 2.3.2](#).

2.1.2.3 Is There a Difference Between a “Dye” and an “Organic Semiconductor”?

Before discussing this topic, we may try to define properly these two terms. The first organic lasers were developed in the mid 60's by Sorokin and Lankard [15] in liquid solutions and called “dye lasers”. The term “dye”, inherited from the chemical and textile industry, was at that time used to designate any kind of luminescent π -conjugated system [16], but used in practice only for highly-luminescent small molecules in organic solvents. Organic electronics later emerged together with the notion of organic semiconductor (OSC), which embraces a much broader family of materials, in particular luminescent conjugated polymers. The term of OSC actually refers to any kind of conjugated system where charge carriers are able to travel from a π -system to another, even though this should happen with a low mobility: this means that the π orbitals of two neighbouring sites have to overlap in some way. The term OSC hence describes a large class of materials but does *not* comprise conjugated systems in solution, either liquid or solid, where emitters are disseminated in a nonconductive medium, i.e. a liquid solvent or a polymer such as polymethyl methacrylate (PMMA) for instance. Lasers based on the latter are still referred to as “(solid-state) dye lasers” in the literature [17]. Everyday use reveals that it is uncommon to hear of a conjugated polymer or an organic crystal as a “dye”. Conversely fluorescent small molecules are equally referred to as “dyes” or OSCs, depending whether they are used disseminated within a host matrix, or in pure *neat films*, respectively. In general, it is observed that small fluorescent molecules that are highly luminescent in dilute form become non-emissive in neat films because of the concentration quenching phenomenon (see [Sect. 2.4](#)). However, there are numerous examples of molecules where this is not the case, for example many emitters used in Organic Light-Emitting Diodes (such as N'-diphenyl-N,N'-bis(1-naphthyl)(1,1'-biphenyl)-4,4'-diamine known as NPB, or Tris(8-hydroxyquinolinato)aluminium known as Alq₃, both used in the first generation of OLED devices). In these cases, as far as quenching does not totally hinder light emission, the distinction between dye and OSC becomes rather irrelevant. A more detailed discussion on this terminology can be found in [18] and is discussed from the point of view of materials classification in [Sect. 3.1.2](#).

2.2 Photophysical Properties of Pi-Conjugated Systems

2.2.1 Absorption of Light by Pi-Conjugated Systems

2.2.1.1 Energy States Involved in Optical Transitions

Optical transitions associated with *single* bonds are of the type $\sigma\text{--}\sigma^*$ and correspond to absorption bands at wavelengths below 160 nm: the related photon energy (>7 eV) is higher than the dissociation energy of most other chemical bonds, meaning that photochemical decomposition is likely to occur, making such compounds not suitable for laser action. Most of laser materials will consequently be based on $\pi\text{--}\pi^*$ transitions. In some molecules, non-bonding orbitals are present, denoted as n orbitals. A typical example is carbonyl compounds where there are two electrons in the non-bonding 2p orbitals of the oxygen atom. Absorption of radiation can occur in a $n\text{--}\pi^*$ transition, i.e. from a “localized” bond to a delocalized bond.

For a convenient description of photophysics, energy states are labeled depending on an important parameter, the spin multiplicity. As described in more detail in [Sect. 2.3](#), electrons have spin angular momentum, described by a spin quantum number $s = \pm\frac{1}{2}$. The sum of all spins of all electrons involved in a system defines the spin S of the system, and spin multiplicity is defined as $2S + 1$. When $S = 0$ the state is said to be a singlet state; when $S = 1$, the multiplicity is 3 and the state is said to be a triplet state.

Excited states in organic materials are created upon absorption of a photon, that is promoting one of the two electrons of the ground state to one empty higher-lying orbital. As inner, filled, energy states are not involved in optical processes, the ground state of the system is usually described by a single filled orbital (the HOMO) containing two electrons, whose spins are necessarily antiparallel in order to comply with the Pauli exclusion principle. As a consequence, the ground state of an organic system is almost always a singlet state, and is denoted as S_0 . A notable exception is molecular oxygen, whose ground state is a triplet state, since in this quite exceptional case, the ground state results from two unpaired electrons in degenerate orbitals.

Excited states are described by two electrons: one residing in the HOMO level, the other one in another antibonding molecular orbital, which may be the LUMO or any another higher-lying antibonding orbital. Because the two electrons are not any more in the same electronic level, Fermi exclusion principle does not hold any more and all spin combinations are possible. The singlet excited states are labeled S_1 , S_2 , etc. and the triplet excited states are referred to as T_1 , T_2 , etc.

Not all optical transitions are possible, they are restricted by optical selection rules [19]. The most important in organic photonics is the *spin selection rule*: for a pure electric dipolar transition, the electric field of the incoming radiation is not able to switch the spin of an electron, so that absorption from the ground singlet

state S_0 can only lead to excited singlet states S_1, \dots, S_n . Creating triplets is not though totally forbidden, and can be enhanced through spin–orbit coupling. Refer to Sect. 2.3 for more details.

Other selection rules are the orbital symmetry selection rule (the two orbitals describing the ground and the excited state must resemble each other), and the parity rule (only transitions between states with different parities are allowed). More details can be found for example in [20].

2.2.1.2 The Energy Band Gap in Pi-Conjugated Systems

Light absorption by conjugated systems can be understood qualitatively with a simplified quantum–mechanical model, such as the free-electron gas model [16]. This simple analogy is illustrated in Fig. 2.4 with the simplest possible linear conjugated system, *S-trans* 1,3 butadiene (C_4H_6). The molecule is planar; carbon atoms connect with other C atoms and with the six hydrogen atoms through three σ -bonds each, meaning that there is a total of 18 sigma Molecular Orbitals (Nine MO of type σ occupied by two electrons, and nine unoccupied σ^* orbitals) for which the highest probability to find the electrons occurs within the molecular plane containing the nuclei (single bonds).

In contrast, the four remaining π -electrons occupy orbitals with one node in the plane of the molecule, and form a charge cloud above and below this plane. It is informative to interpret the two lobes (and the related zero probability to find a pi-electron in the molecular plane) as the result of a destructive quantum interference, evoking the $n_z = 2$ quantized mode of a quantum box in the z -direction (see Fig. 2.4): they represent a mode with one node at the center, having opposite signs of the wavefunction on the two sides. The box modes represented in Fig. 2.4 are strictly valid for a constant potential inside the box which is obviously not the case especially in the plane of the molecule, but the physical contents remain. Thus, with the simple picture of a rectangular box with infinite walls, the four pi-orbitals plotted in Fig. 2.4 resemble the four first quantized modes $n_x = 1, 2, 3, 4$ with the fixed quantum numbers $n_z = 2$ and $n_y = 1$. A linear conjugated system appears as a nanowire with discrete energy levels due to confinement. If we simplify a little bit further and consider a linear molecule as a 1D system of length L , then the energy $E(n)$ of the n th eigenstate is given by

$$E(n) = \frac{h^2 n^2}{8m_e L^2}$$

where n is the quantum number (equal to the number of antinodes along the chain), m_e the mass of the electron, h the Planck's constant. When some light is incident upon a conjugated molecule, an optical transition occurs between a filled orbital and an empty one. The lowest photon energy enabling such a transition defines the *optical gap*, which is somewhat lower than the *HOMO–LUMO* gap. The latter is defined as the energy difference between the **H**ighest **O**ccupied **M**olecular **O**rbital

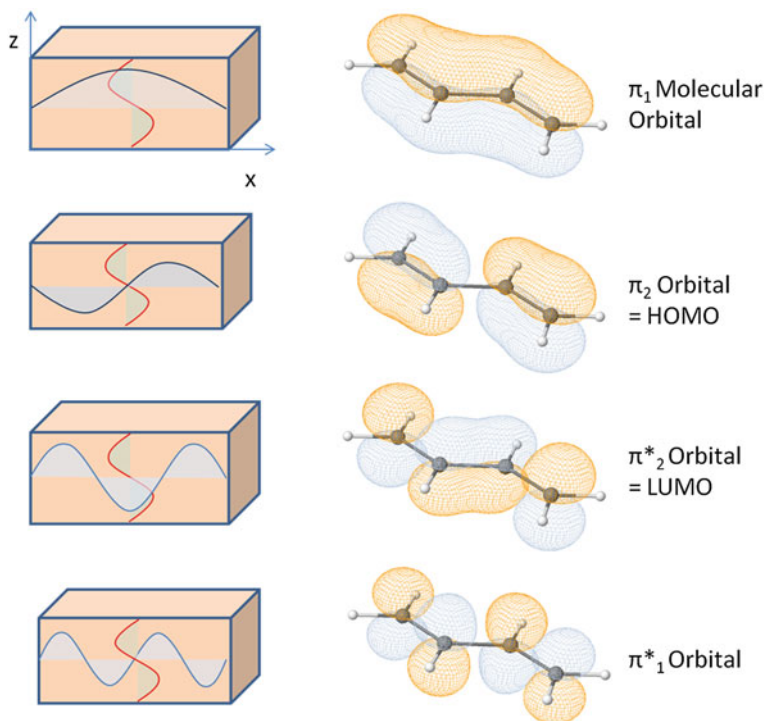


Fig. 2.4 Analogy between the electronic levels of a free electron in a rectangular quantum box with infinite walls (*left*), and the pi molecular orbitals of *S-trans* 1,3-butadiene, calculated with Orbimol® [21]. The pi molecular orbitals correspond to a zero probability to find the electrons within the molecular plane; in the quantum box model, although this corresponds to the nonrealistic case of a constant potential inside the box, π -orbitals can be ascribed to $n_z = 2$ modes (one node in the plane cutting the box in two parts in the z -direction), the σ orbitals corresponding to $n_z = 1$. Since butadiene contains 4 pi-electrons, they occupy by pairs the two first π_1 and π_2 orbitals, which are associated to $n_x = 1$ and $n_x = 2$, respectively, where n_x is the number of antinodes in the longest direction of the quantum box. The LUMO and LUMO + 1 levels, empty in the ground state, correspond to the $n_x = 3$ and $n_x = 4$ modes

(HOMO) and the **Lowest Unoccupied Molecular Orbital (LUMO)**; the difference between the HOMO–LUMO gap and the optical gap arises from the attractive interaction existing between a hole (absence of electron in HOMO) and an electron (supplementary electron in LUMO) when they coexist in a single molecule to form the excited state; this is actually the exciton binding energy evoked above, added to the exchange energy specifically for triplet states (see Sect. 3). However we neglect for the moment this difference for the sake of simplicity. Generally the number of *pi*-electrons N is an even number (this is true for stable molecules, notable exceptions are polarons, or charge carriers, in OSCs) which means that the

$N/2$ first π orbitals are full, up to the HOMO orbital included, and the $N/2$ upper π^* -orbitals are empty starting from the LUMO. Then the energy gap writes:

$$E_{\text{gap}} = E(\text{LUMO}) - E(\text{HOMO}) = E\left(n = \frac{N}{2} + 1\right) - E\left(n = \frac{N}{2}\right) = \frac{h^2(N+1)}{8m_e L^2}$$

This minimal energy gives the longest wavelength that can be absorbed, through the relation:

$$\lambda_{\text{max}} = \frac{hc}{E_{\text{gap}}} = \frac{8m_e c L^2}{h(N+1)}$$

This indicates that within a good approximation the position of the absorption band is determined by the chain length L and the number of π -electrons N only. In the example of butadiene, $E_{\text{gap}} = 9.73$ eV (calculated from HOMO–LUMO levels [21]), which yields with $N = 4$ an expected chain length $L = 4.4$ Å. Each of the three bonds in *S*-trans-butadiene is 1.35 Å long, meaning that there is a fair agreement between the simple theory and the experimental values provided that the chain length L extends beyond the terminal atoms by only 0.18 Å on both sides. In general, there is a correct match for linear simple dyes (e.g. cyanines [16]) but in most practical cases unfortunately the relationship between chemical structure and absorption spectrum is not so simple.

For benzene for instance, in which the six *pi*-electrons are fully delocalized above and below the six carbon atoms, naïve pictures do not work so well: attempting to retrieve the energy gap from the circumference of the ring (let's say, in a similar fashion as we do in the Bohr model to retrieve the electronic levels of the hydrogen atom) leads to large errors because the repulsion force between the six electrons is strong and plays a prominent role [16].

From this simple picture however we can approach how it is possible to tailor the spectral properties of pi-conjugated systems. It appears relatively easy to modify the absorption spectrum (and in a closely related way, the emission spectrum) by varying the chemical structure. This sets a huge (and very useful in practice) difference with inorganic semiconductors where the emitted wavelengths are strongly limited by the available materials and by lattice-matching restrictions.

There have been many efforts made over the past decades, in molecular engineering, to achieve such a “bandgap engineering” of *pi*-conjugated systems [22, 23]. Playing on the conjugated length is the most straightforward way, as illustrated in the polyacene series, where the adjunction of phenyl rings from benzene to pentacene leads to a redshift of absorption spectrum [24]. It is not the only way to tune the bandgap: another efficient strategy (illustrated in Fig. 2.5) consists in incorporating Electron Withdrawing Groups (EWG) like keto, cyano or dicyano groups which tend to lower the LUMO energy level, or conversely to attach Electron Donating Groups (EDG) such as alkyl, alkoxy or alkylsulfanyl

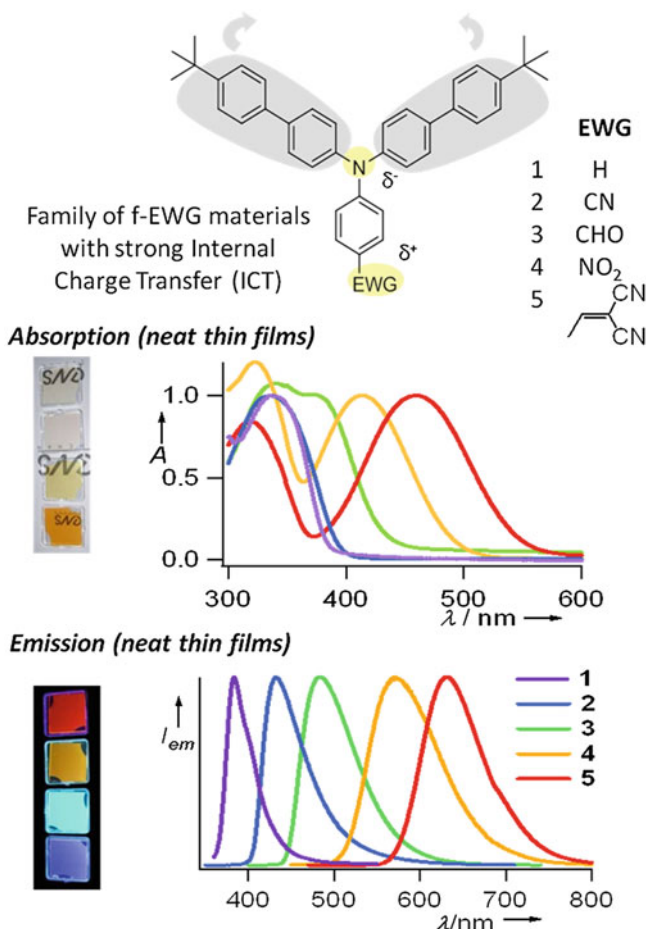
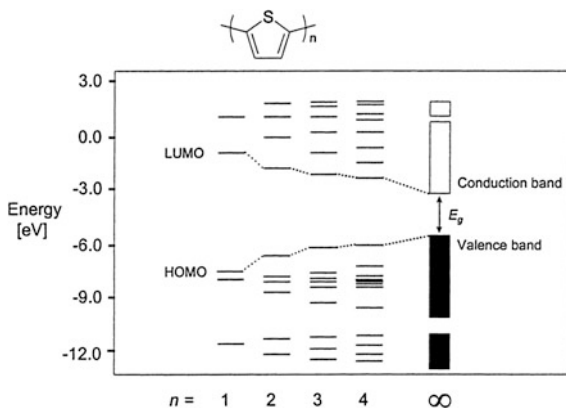


Fig. 2.5 Illustration of bandgap engineering and chemical tuning by substitution of different Electron-Withdrawing Groups (EWG) on a triphenylamino moiety. The EWG are labeled from 1 to 5 from the lowest electron-accepting to the highest electron-accepting character. The more the EWG attracts electrons, the lower the bandgap and the more the absorption and emission are redshifted. Absorption and fluorescence spectra of 100-nm-thick evaporated neat films are shown. The strong light emission by neat solid films of dye molecules is a rather uncommon feature, because in general concentration quenching prevents emission. Here it can be explained by several factors: low π -stacking thanks to steric hindrance of tert-butyl terminal groups and a twist of the triphenylamino core, as well as a strong Stokes shift preventing intermolecular dipole-dipole or radiative energy exchange. Courtesy of E. Ishow. Reprinted with permission from [3]. Copyright (2008) American Chemical Society

groups which tend to elevate the HOMO energy level [23]. In both cases the tendency is to lower the bandgap. The spectral limits to the UV and to the IR of bandgap engineering are discussed in Sect. 3.2.

Fig. 2.6 Calculated (frontier) energy levels of oligothiophenes with $n = 1-4$ and of polythiophene, where E_g = band gap. Courtesy of E.W. Meijer. Reprinted from [100], Copyright (2001), with permission from Elsevier



2.2.1.3 Absorption Spectra

Origin of Broad Spectra

A striking peculiarity of the absorption spectra of organic systems, as opposed to atomic/ionic spectra, is the width of the bands, usually covering several tens up to a hundred nanometers. The large number of electronic individual π -orbitals shared in a π -conjugated system tends to form “bands”, as sketched in Fig. 2.6 for the typical example of oligothiophenes.

However this image of band formation does not explain completely why absorption spectra are *continuously* broad, and not formed of multiple sharp peaks that we could resolve with a high-resolution spectrometer, for instance, especially for small molecules where the number of shared π orbitals is not so large.

It becomes clear when one considers that even a small dye molecule (such as DCM, represented in Fig. 2.6) contains several tens of atoms, with at least a hundred or more associated vibration modes of the molecular skeleton. These vibrations of the nuclei densely cover a spectrum between a few cm^{-1} to $\sim 3000 \text{ cm}^{-1}$. Indeed, it is useful to keep in mind that when a simple classical oscillator (e.g. a spring) with a given natural resonance frequency is coupled to an identical resonator (through a loose spring for instance), then the two coupled resonators have two eigenmodes whose eigenfrequencies are separated by an amount representing the strength of the coupling [25]; here the numerous possible vibrations inside a molecule couple each other and give birth to a dense ladder of closely-spaced vibrational states. These vibrational states are coupled to electronic states, so that each electronic state is in fact a set of closely-spaced *vibronic* levels, since basically the energy of an electron in a molecular orbital depends on its position with respect to the nuclei, which are all subject to vibrational motion. For completeness, let's add that each vibrational level is broadened by the existence of many close rotational levels (the term ro-vibrational level is hence used to described the coupled states), and that a large molecule has many geometrical

conformations, each of which being associated to a slightly different position of the resulting vibronic levels. As a result the spectra of dye molecules and organic semiconductors are very broad (~ 100 nm) and continuous, which makes them very valuable for tunable lasers.

Homogeneous Broadening

An important aspect of this broadening related to laser applications is its nature. In organic systems *the broadening is homogeneous*, meaning that all molecules taken individually have the same spectrum than the ensemble, so that every molecule can contribute equally to the building of a given oscillating laser mode. Stated differently, the broad bands observed in *pi* systems do not result from the superposition of many narrow lines coming from different emitters, like it is the case for instance in a Doppler-broadened gas medium, where contributions to the gain at a given wavelength is ascribed to a class of molecules having a given velocity in the gas. However there may exist some sources of inhomogeneous broadening, resulting from the conformation distribution and from variations of the local environment seen by the chromophore.

Absorption Cross Sections

Absorption is usually quantified by the absorption coefficient α (in cm^{-1}) or preferably by the *absorption cross section* $\sigma_{abs} = \alpha/N$, a figure which is however meaningful only if the density of absorbing units N (in cm^{-3}) is well defined or can be estimated. The absorption cross section relates to a single molecule, it has the dimensions of a surface (usually expressed in cm^2) because it represents the effective area of the molecule as if the latter were a totally-absorbing planar element of area σ_{abs} set in the path of the beam. The (unsaturated) transmission $T(\lambda)$ of a homogeneously absorbing sample of length L is simply given by:

$$T(\lambda) = \exp[-\alpha(\lambda)L] = \exp[-\sigma_{abs}(\lambda)NL] = 10^{-A(\lambda)}$$

where A is the absorbance (usually defined in base 10, with $A = \varepsilon(\lambda) cL = \frac{\alpha(\lambda)L}{\ln(10)}$, where $\varepsilon(\lambda)$ is the molar absorptivity in $\text{M}^{-1} \text{cm}^{-1}$ or liters/(mol cm), and c the concentration in M). Note that the validity of the Beer-Lambert law is restricted to linear absorption in absence of stimulated emission.

Although this is not the most convenient unit for a laser physicist, the molar absorptivity ε is often found as a measure of absorption of molecular systems in the literature, and is simply connected to the absorption cross section by:

$$\sigma_{abs}[\text{cm}^2] = \frac{1000\ln(10)}{\mathcal{N}_A} \varepsilon[\text{l mol}^{-1} \text{cm}^{-1}] = 0.385 \cdot 10^{-20} \varepsilon[\text{l mol}^{-1} \text{cm}^{-1}]$$

where \mathcal{N}_A is the Avogadro number.

Experimental determination of absorption coefficients $\alpha(\lambda)$ is straightforward. It is evaluated from the spectral transmission measurement $T(\lambda)$ performed with a spectrophotometer operating at low intensity input light levels to work in the linear absorption regime. Absorption cross sections can then be derived as far as the chromophore density N is known. The latter parameter is simple to estimate in the case of dye-doped polymer films: the exact amount of dye in the film is deducible from the mass doping ratio x and the density of the film ρ . The latter can be reasonably approximated to the density of the undoped polymer film, as far as the doping ratio does not exceed a few percents. The dye density is then equal to:

$$N = \frac{x\rho\mathcal{N}_A}{M}$$

where M is the molar mass of the dye. From this relationship we can derive the useful following relation, which enables computing the absorption cross section of a dye molecule directly from the absorbance measurement of a polymer film or rod of density ρ and length L , doped at a mass ratio x with a dye of molar mass M :

$$\sigma_{abs} [cm^2] = \frac{M[g\ mol^{-1}]A(\lambda)\ln(10)}{x\mathcal{N}_A\rho[g\ cm^{-3}]L[cm]}$$

In organics the absorption cross sections are large, typically on the order of $\sigma_{abs} \sim 10^{-15}\ cm^2$. They are comparable or might be slightly lower than absorption cross sections for interband transitions in inorganic semiconductor quantum dots (typically $>10^{-14}\ cm^2$ [26]), but they are considerably larger than cross sections of rare-earth ions in crystalline laser media, which are usually based on metastable transitions that are forbidden in nature, and happen to be allowed in a solid-state environment in virtue of the coupling with the solid matrix; thus, in Neodymium, Ytterbium or Erbium based lasers, cross sections are only¹ typically $\sim 10^{-19}\ cm^2$.

In conjugated polymers or organic crystals, the density of active units or the number of chromophores per chain is not precisely known; in these cases the absorption coefficient α might be more relevant to quantify absorption than the absorption cross section. α has typical values of 10^4 – $10^5\ cm^{-1}$ at the peak absorption wavelength in organic solids, which is comparable to values measured in bulk inorganic semiconductors for interband transitions near the band gap [27].

In the case of neat films ($x = 1$) of evaporated small molecules, N is of the order of $N \approx \rho \times N_A/M = 1.3 \times 6.10^{23}/460 \sim 10^{21}\ cm^{-3}$ where ρ is the film density (numerical values here are those of Alq₃ [28]), which means that the

¹ Although this low absorption cross section is also associated to a low emission cross section (and hence a low gain), this does not mean that crystalline gain media doped with rare-earth ions would be “worse” than organics or semiconductors to make a good laser material, because the metastability of the excited state also means that Nd, Yb or Er ions have a very long lifetime ($\sim ms$), enabling a good energy storage capability. For this reason population inversion is easy to reach in rare-earth ions, even in three-level (Er) or quasi-2 level (Yb) configurations.

incident light will be absorbed over a typical length scale of $L_{abs} = \alpha^{-1} = (\sigma_{abs}N)^{-1} \sim 100$ nm. This is also the typical order of magnitude for a film of conjugated polymer like PFO or PPV. This value is noticeably lower than the optical wavelength, which will have some impact on the laser resonator design (see Chap. 4).

For theoretical work on lasers based on conjugated polymers, it may be however useful to know the absorption cross section. In this case, it is possible to derive it indirectly, by measuring first the fluorescence quantum efficiency and the radiative lifetime, and then obtaining the absorption cross section using the Strickler–Berg formula exposed later in Sect. 2.4 [29].

The Transition Dipole Moment

The absorption cross section spectrum is not the single figure needed to properly quantify absorption in organic *pi*-conjugated systems; indeed absorption is fully described by a vectorial quantity, the transition dipole moment.

The absorption transition dipole from the ground state g to an excited state e is defined by [30]:

$$\vec{d}_a(g \rightarrow e) = \left\langle \psi_g | \tilde{\vec{d}}_a | \psi_e \right\rangle$$

where ψ_f and ψ_e are the stationary wavefunctions of the involved states, and $\tilde{\vec{d}}_a$ is a vector operator being the sum of the position vectors of all charged particles weighted with their charge. According to the Franck–Condon principle, absorption is a fast process and the positions of the nuclei are thus assumed to be fixed, so that only the electronic part of the wavefunctions is affected during the absorption of a photon. In the most simple and archetypal case of a dye planar aromatic molecule with a $S_0 \rightarrow S_1$ transition having a $\pi-\pi^*$ character, both ψ_g and ψ_e orbitals are symmetrical with respect to the plane of the molecule, so that the integral defining \vec{d}_a along the direction perpendicular to this plane is zero, since the integrated function is odd. Hence $\vec{d}_a(S_0 \rightarrow S_1)$ lies in the plane of the molecule. If the dye is pumped in its S_2 state, the excited wavefunction involves in general a π^* orbital as well, and $\vec{d}_a(S_0 \rightarrow S_2)$ remains in the plane of the molecule. However the profile of the π^* orbitals in the plane are different, and thus their corresponding transition dipoles are not oriented similarly.

In the case of a “rod-like” or linear molecule such as DCM (see Fig. 2.7) the absorption transition moment will be along the molecule axis [31]. In polyacenes (naphthalene, anthracene...) the $S_0 \rightarrow S_2$ moment is perpendicular to the $S_0 \rightarrow S_1$ moment, the latter being along the axis connecting the phenyl rings [32]. This is also the case of fluorescein-based molecules represented in Fig. 2.8.

In optical experiments, this feature means that a molecule will respond differently according to the polarization state of the incoming radiation. In solid films

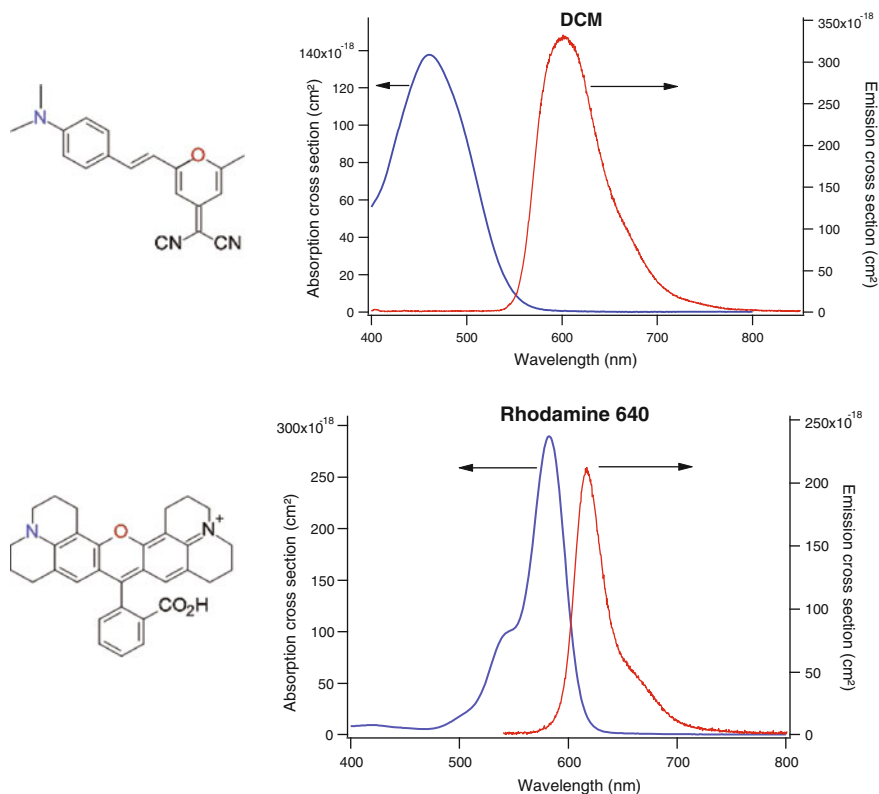


Fig. 2.7 Absorption and emission cross-section spectra of DCM and Rhodamine 640 in PMMA

where molecules are not randomly oriented, this causes the absorption to be polarization-dependant [33].

2.2.2 Emission of Light by π -Conjugated Systems

2.2.2.1 Emission Spectra

Let's now examine the fate of a molecule after absorbing a photon of energy $h\nu$. Absorption occurs between the lowest-lying vibrational state of the S_0 electronic state and a vibronic subband of the S_1 or S_2 excited singlet states, as selection rules make the singlet-to-triplet transitions forbidden, and therefore associated to very low absorption cross sections compared to singlet-to-singlet transitions.

Like absorption spectra, emission spectra are broad and have a typical width at half maximum of several tens of nm. This broad fluorescence leads to a possible tuning of the emission wavelength, thanks for instance to a dispersive element

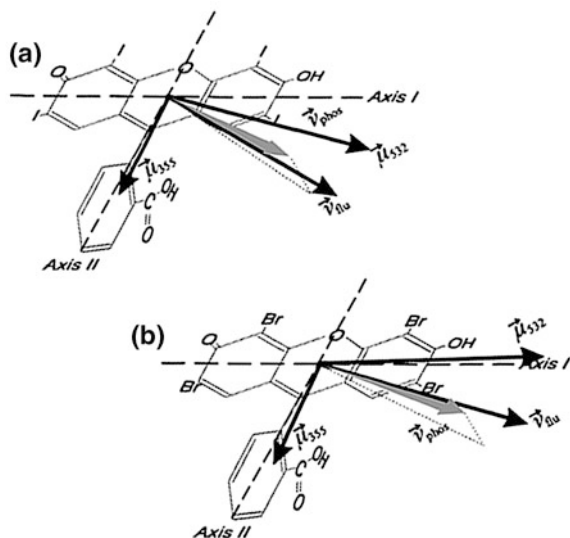


Fig. 2.8 Illustration of the difference which may exist in the orientation of dipole transition moments, depending on the wavelength of excitation. The two examples correspond here to phosphorescent small molecules with a fluorescein core and I or Br substituents. The dipole moment of absorption is featured for an absorption wavelength of 532 nm ($S_0 \rightarrow S_1$ transition) and at 355 nm ($S_0 \rightarrow S_2$ transition), and they appear to be almost orthogonal. The transition dipole for emission (fluorescence or phosphorescence) is aligned with none of the absorption moments. Courtesy of P. Lettinga. Reproduced from [101]

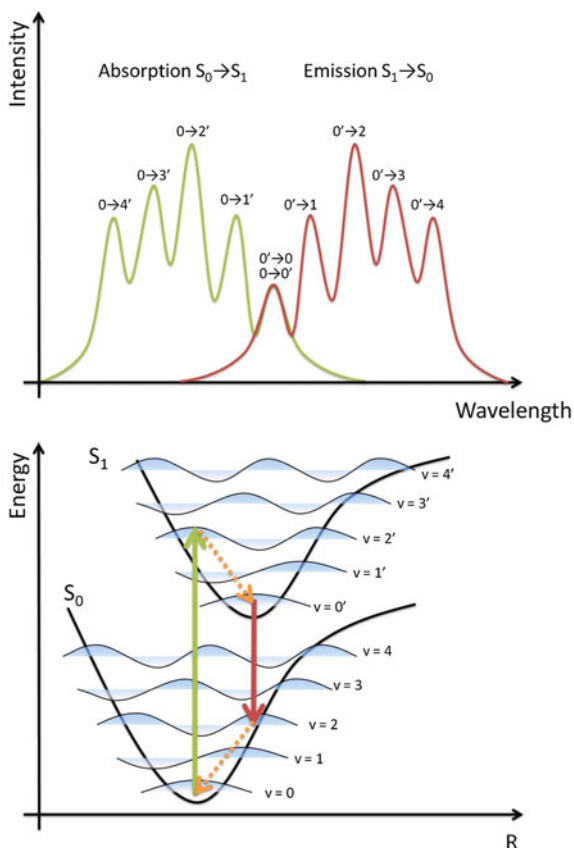
added inside the laser cavity [34], and also makes them capable of ultrashort pulse generation [35].

A key point for organic laser physics resides in the existence of a large *Stokes shift* in organic materials, i.e. a redshift of the emission compared to the absorption.

In virtue of the Franck–Condon principle [36]² the electrons in a molecule are supposed to move much faster than the nuclei, because of their much lower mass. Hence, when a molecule absorbs a photon, with a timescale of 10^{-15} s, the entire molecular structure takes some time ($\sim 10^{-12}$ s) to relax and thermalize to the minimum vibronic level of a S_1 state whose minimum lies at a higher normalized nucleus coordinate r . A physically-intuitive picture of such a relaxation can be drawn with the simple example of the H_2 molecule, explained in many elementary

² “Classically, the Franck–Condon principle is the approximation that an electronic transition is most likely to occur without changes in the positions of the nuclei in the molecular entity and its environment. The resulting state is called a Franck–Condon state, and the transition involved, a vertical transition. The quantum mechanical formulation of this principle is that the intensity of a vibronic transition is proportional to the square of the overlap integral between the vibrational wavefunctions of the two states that are involved in the transition”—IUPAC Compendium of Chemical Terminology, 2nd Edition (1997).

Fig. 2.9 Illustration of the Stokes shift and mirror symmetry of absorption and emission spectra. The molecular potentials are sketched as a function of R , a spatial coordinate linked to the position of the nuclei. Vibronic eigenstates are denoted by v and v'



textbooks [36, 37]. In an energy E versus r (nuclear coordinate) diagram, optical transitions then occur vertically, as sketched in Fig. 2.9, where the typical Morse-shaped molecular potentials reminds us that at high vibrational levels the stretching of bonds can lead to molecular dissociation. As explained above spectra recorded at room temperature do not allow resolving the vibronic levels in typical systems, but at cryogenic temperatures, one may observe sharp peaks and check for the “mirror-image” symmetry property between absorption and emission spectra [16].

Typical examples of absorption/emission spectra are given at room temperature in thin solid films of PMMA in Fig. 2.7 for two well-known red emitting organic dyes, namely Rhodamine 640 and DCM.

2.2.2.2 A 4-Level System (At First Sight)

For lasers, the direct consequence of the existence of a Stokes shift is that *organic lasers are at first approximation 4-level systems*. The presence of higher-lying

singlet states (allowing for excited-state absorption), triplet states, and in some cases polaron states makes the medium more complex but the approximation of a 4-level system is satisfactory in many cases. The rapidity of the intraband decay (\sim ps) explains why the fluorescence spectrum does not depend on which sub-level (within the S_1 manifold) the molecule has been excited. Excitation in a higher level S_n ($n > 1$) also leads to the same emission spectrum, as internal conversion from S_n to S_1 also occurs on a picosecond scale through nonradiative processes. Pumping to a S_n state ($n > 1$) leads to heat dissipation through these nonradiative channels, and is consequently detrimental to the laser efficiency. The lower-lying vibronic level of S_1 has a “long” lifetime, typically a few nanoseconds, and is from this point of view an adequate upper lasing level. The lasing transition then occurs between this level and one of the ro-vibrational levels of the S_0 manifold, before another fast nonradiative decay brings the molecule back to the ground state, i.e. the lower-lying level of S_0 .

For laser applications, a large Stokes shift is desirable as it minimizes the amount of ground state reabsorption of laser light and makes it closer to a true four level system. A too high Stokes shift is not ideal though, as it enhances the thermal loading and sends the molecule in a highly-excited vibrational state which is more likely to lead to photodissociation.

The extent of the Stokes shift for a given *pi*-conjugated compound is highly dependent on the environment (host matrix) and particularly on its polarizability: the higher the polarizability of the surrounding, the higher the redshift [32]. This well-known effect in molecular fluorescence means for example that when a dye molecule with a high polarizability is dispersed into a nonpolar host matrix, the emission curve will shift towards longer wavelengths upon increasing the dye concentration. An example of such a behavior can be seen in triarylaminates in Alq₃ [38].

2.2.3 Jablonski Diagrams

Photophysical events within a chromophore moiety (flows between energy states for a given dye molecule or chromophore unit in a polymer) can be sketched with the help of molecular potentials as presented in Fig. 2.10. Plotting the vibrational ladders inside the typical Morse potentials would be helpful for the understanding of some photodissociation effects occurring when molecules are excited to highly-excited vibrational states for instance. However, experimental access to the exact shape of these potentials is impossible in virtue of the numerous geometrical conformations of one molecule in a solid, each conformation being associated to one molecular potential. A simpler and much more widespread picture consists in drawing the energy levels as simple horizontal lines, in a Jablonski diagram (see Fig. 2.11).

Two groups of electronic states exist: singlet states (S_0, S_1, \dots, S_n) which have a total spin of zero, and triplet states (T_1, T_2, \dots, T_n) which have a total spin of one.

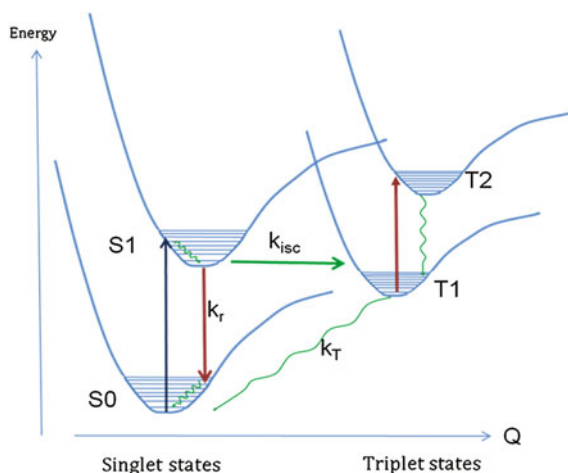


Fig. 2.10 Energy level diagram relevant for organic dyes versus a normalized nucleus coordinate Q . The shift in Q between singlet and triplet states is pictured for clarity only. In organic semiconductors more complex intermolecular (or intrachain) interactions occur. Lasing occurs on the singlet $S_1 \rightarrow S_0$ transition, where stimulated emission (SE) can efficiently bypass the radiative spontaneous emission occurring with a rate k_r . Intersystem crossing (ISC) causes triplet states T_1 to be generated from S_1 states. Since their (nonradiative) decay rate k_T is small, they accumulate until they totally hinder SE through a dipole-allowed efficient $T_1 \rightarrow T_2$ absorption (Triplet absorption), or through other nonradiative energy transfers (Singlet–Triplet or Triplet–Triplet Annihilation)

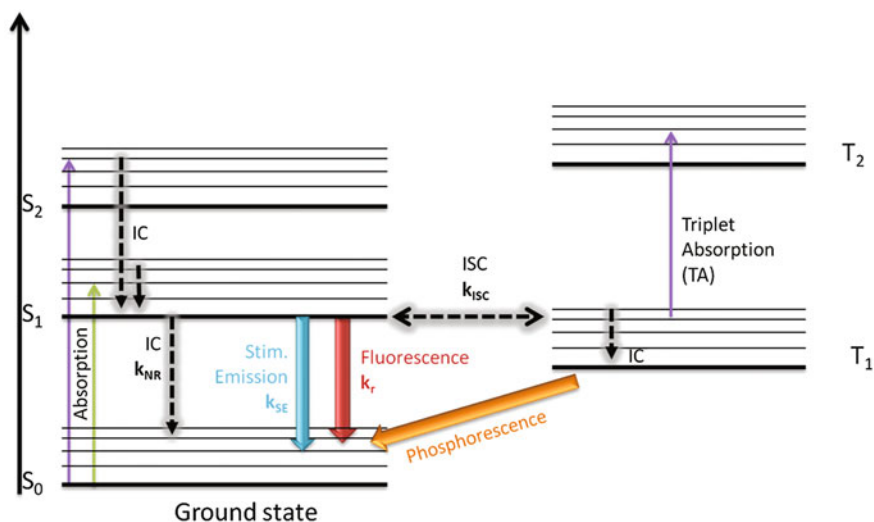


Fig. 2.11 A Jablonski diagram featuring the ground state (lowest vibrational level of the S_0 manifold), the singlet S_1, S_2, \dots and triplet T_1, T_2, \dots excited states. Nonradiative decay occurs within the vibrational levels of a given electronic level, or from S_2 to S_1 for instance, through Internal Conversion (IC). Intersystem Crossing (ISC) occurs between S_1 and T_1

Triplet states play an especially important role in the understanding of organic lasers, and will be discussed with more details in [Sect. 2.5](#).

Once a molecule has been promoted to the S_1 state, either directly from the ground state or after internal conversion (IC) from a higher S_n state, it first decays down to the lowest vibrational state by a rapid Internal Conversion process, which occurs within $\sim 10^{-14}$ – 10^{-10} s, then the molecule is deexcited through different possible mechanisms, briefly described below.

2.2.3.1 Fluorescence

The molecule can decay radiatively through **fluorescence**: the radiative decay is given by $k_r = \tau_{rad}^{-1}$ where τ_{rad} is the radiative lifetime, which is fundamentally connected to the absorption of the $S_0 \rightarrow S_1$ band through the Einstein relations. However as the latter apply strictly speaking to atomic systems with sharp lines, a modified formula is needed in practice to take into account the broad nature of absorption and emission: Strickler and Berg [39] derived the following useful relation connecting the radiative lifetime to the absorption cross section spectrum [40]:

$$\begin{aligned} k_r &= \frac{1}{\tau_{rad}} = \frac{8\pi c n_F^3}{n_A} \frac{\int_{S_0 \rightarrow S_1(em)} f(\lambda) d\lambda}{\int_{S_0 \rightarrow S_1(em)} f(\lambda) \lambda^3 d\lambda} \int_{S_0 \rightarrow S_1(abs)} \frac{\sigma_{abs}(\lambda)}{\lambda} d\lambda \\ &= \frac{8\pi c n_F^3}{n_A \langle \lambda^3 \rangle_F} \int_{S_0 \rightarrow S_1(abs)} \frac{\sigma_{abs}(\lambda)}{\lambda} d\lambda \end{aligned}$$

In this expression, n_A (resp. n_F) is the average refractive index of the material in the absorption (resp. emission) spectral region ($n_A > n_F$). The average of λ^3 appears denoted as $\langle \lambda^3 \rangle_F$, weighted by the fluorescence spectrum $f(\lambda)$; the latter integral is theoretically restricted to the $S_1 \rightarrow S_0$ emission region, but in most practical cases the whole emission spectrum is only ascribed to fluorescence from S_1 hence no special care has to be taken for the integration boundaries. Conversely, a higher care must be paid to the integral over the absorption spectrum, restricted to the $S_0 \rightarrow S_1$ band: it does not include the absorption to higher energy levels (S_n states) occurring at lower wavelengths. In general, $S_0 \rightarrow S_1$ and $S_0 \rightarrow S_n$ bands can be clearly distinguished in the absorption spectrum.

2.2.3.2 Internal Conversion

The molecule can decay nonradiatively directly to the ground state by **internal conversion (IC)**, with a nonradiative decay rate $k_{nr} = \tau_{nr}^{-1}$. A general rule of thumb relates the importance of nonradiative decay by IC to the structural rigidity of the molecule: as nonradiative decay requires some kind of vibrational coupling between the excited and the ground state, rigid and planar molecular structures will

tend to favor luminescence versus IC, as illustrated in the highly fluorescent fluorescein molecule [16]. Internal conversion is favored when a resonance is found between a highly vibrational state of S_0 and the lowest-lying vibronic state of S_1 : for this reason stretching vibrations associated to hydrogen atoms, which are highly energetic because of the low mass of the hydrogen atom, are likely to contribute to nonradiative decay (see e.g. the case of Rhodamine 110 [16]). Also for this reason long-wavelength emitters with a small energy gap are more likely to suffer from internal conversion (this effect is a result of the “energy gap law”, see Sect. 2.2.5.) For green, blue or UV-emitting molecules however, a quantum yield of fluorescence <1 is rather attributed to ISC rather than IC (see below).

2.2.3.3 Intersystem Crossing

The molecule can transfer its excitation to the long-lived triplet state T_1 by **intersystem crossing (ISC)**, with a rate k_{ISC} . This phenomenon, which primarily depends on the extent of spin–orbit coupling in the molecule, is described with more details in the following (cf. Sect. 2.3.3).

Once a molecule has been transferred to the triplet state T_1 , it may relax to the ground state with a rate $k_T = \tau_T^{-1}$ which is mostly a pure nonradiative decay because the T_1 – S_0 transition is spin-forbidden. Radiative decay from the T_1 state is referred to as phosphorescence, it can be observed at low temperatures when vibrational excitations are frozen, or for molecules exhibiting a strong spin–orbit coupling. An emitter in the T_1 state may also be promoted to a higher-lying triplet state T_n by a spin-allowed transition, this is called **triplet absorption (TA)**, with typical cross section $\sigma_{TT} \sim 10^{-16} \text{ cm}^2$, or decay to the ground state in a bimolecular process through the encounter with a singlet state or a triplet state, by **singlet–triplet annihilation (STA)** or **triplet–triplet annihilation (TTA)** respectively. As triplet states and bimolecular phenomena play an important role in the physics of organic lasers, they are treated with more details in Sects. 2.5 and 2.6 of this chapter, respectively.

A useful figure-of-merit of organic emitters is the *quantum yield of fluorescence* ϕ_F ($0 < \phi_F < 1$). It is defined as the ratio of emitted fluorescence photons divided by the number of absorbed pump photons. This parameter is sometimes defined with additional quenching terms at the denominator (representing other nonradiative decay pathways for S_1 population), but it does not take into account stimulated emission as a possible decay path, i.e. it is always defined in a non-lasing case ($I = 0$).

$$\phi_F = \frac{k_r}{k_r + k_{nr} + k_{ISC}} = \frac{\tau_{nr}}{\tau_{rad} + \tau_{nr} + k_{ISC}\tau_{rad}\tau_{nr}} = \frac{\tau_F}{\tau_{rad}}$$

$\tau_F = \phi_F \tau_{rad}$ is the fluorescence lifetime, which is actually the measured or the effective lifetime of the singlet state, taking into account all possible sources of decay (except stimulated emission). The fluorescence lifetime is always shorter than the radiative lifetime.

2.2.3.4 Stimulated Emission

The molecule can decay radiatively through **stimulated emission** with a rate $k_{SE} = \sigma_{em}I$ where σ_{em} is the stimulated emission cross section (cm^2), and I the intracavity laser intensity expressed in photonic units (the photon flux per unit area).

2.2.4 Photophysical Parameters Relevant for Organic Lasing

2.2.4.1 The Saturation Intensity I_{SAT}

It is worth noting that the different downward decay rates depleting the S_1 state compete with each other, and among intramolecular phenomena the stimulated emission rate is the only one to be intensity-dependant. A useful quantity in laser physics is the laser saturation intensity defined as:

$$I_{\text{sat}}(\text{photonic units}) = \frac{1}{\sigma_{em}\tau_F}$$

$$\text{or } I_{\text{sat}}(\text{energetic units}) = \frac{hc}{\lambda_{\text{laser}}\sigma_{em}\tau_F}$$

Organic materials have saturation intensities which are of the order $I_{\text{sat}} \sim \text{MW}/\text{cm}^2$. I_{sat} is the (intracavity) laser intensity for which the stimulated emission rate $\sigma_{em}I$ is equal to the spontaneous decay rate $\frac{1}{\tau_F}$, the latter including all nonradiative decays by IC or ISC. Stated otherwise, $I > I_{\text{sat}}$ defines a lasing operating regime where stimulated emission is the dominant mechanism draining the S_1 population back to the ground state. In this regime, as every photon produced by stimulated emission “kills” one excited molecule to bring it back to the ground state, the population inversion becomes saturated and is very small, in the same (symmetric) fashion as the absorbance of a saturable absorber decreases when the incoming intensity surpasses the saturation intensity.

Let’s clarify one point that is often misunderstood: the saturation intensity is an *intracavity* laser intensity and is not related directly to the pump laser intensity threshold; it is not either an indication of a “maximum” intensity that could be produced by a laser. A laser operating in a pure CW regime, let’s say, is not an energy-storing device but an energy-converting device, converting the energy of the pump into a laser beam. If no additional effects come to complicate the 4-level diagram at high intensities, and if photodegradation issues do not exist, then in this perfect world we could convert the pump light into laser light with no upper limit in pump power, though with a less-than-one efficiency: the output/input intensity characteristic of the laser would be a straight line with a threshold and no upper bound.

Seeking the saturated regime ($I > I_{sat}$) is generally useful in laser systems where nonradiative pathways exist (and limit the efficiency and the photostability), because they can be quenched by stimulated emission. A high laser intensity may be obtained through the design of high-Q cavities for a given pump intensity. The reduction of the triplet formation channel by ISC has been observed when lasing was activated in a polymer laser [41]. The inhibition of spontaneous decay by stimulated emission in organic chromophores has also been exploited in a different context in microscopy, and is known as Stimulated Emission Depletion (STED) Fluorescence Microscopy [42].

2.2.4.2 Stimulated Emission Cross Sections

As organic media have very strong absorption cross sections, they have accordingly comparable stimulated emission cross sections and therefore exhibit optical gains which stand among the highest of all laser media (gain cross sections around 10^{-15} cm^2 are thus typically reported in conjugated polymers [43]) and are comparable with gains met in inorganic semiconductors. The linear gain g (usually expressed in cm^{-1}) is defined as:

$$\frac{dI}{dz} = g = \sigma_{em} \Delta N = \sigma_{em} S_1 N$$

where I is the laser intensity in photonic units (photon flux in $\text{m}^{-2} \text{ s}^{-1}$) and ΔN is the population inversion (m^{-3}) between the upper level and the lower level of the lasing transition. As the latter level is rapidly flushed towards the ground state by internal conversion within picoseconds, the inversion is equal to the S_1 singlet state density. Here we denote as S_1 the relative population of the S_1 state, i.e. $\Delta N = S_1 N$, N being the molecular density. To fix ideas, with a chromophore density N of the order of $\sim 10^{19} \text{ cm}^{-3}$ (dye-doped polymers, guest/host systems) to $\sim 10^{21} \text{ cm}^{-3}$ (neat molecular solids, conjugated polymers), a complete inversion in an otherwise lossless medium would yield gains up to $\sim 10^4$ – 10^6 cm^{-1} .

These very high gains mean that the saturation intensity defined above can be reached in length scales that are of the order of a few mm at most, a limitation that is met when measuring gains by the variable Stripe length technique for instance (see Chap. 3).

Emission cross sections can theoretically be derived from optical gain characterizations (see Chap. 3), however it is not straightforward to measure independently the singlet state population, especially when steady state is not reached (which is often the case in organic lasers operating with short pulses). This is why it is preferred to use the following formula derived from the Strickler–Berg relation [1, 39]:

$$\sigma_{em}(\lambda) = \frac{\lambda^4}{8\pi c n_F^2 \tau_{rad}} \frac{f(\lambda)}{\int f(\lambda) d\lambda}$$

where n_F is the average refractive index in the emission spectral region, $f(\lambda)$ the fluorescence spectrum (in arbitrary units because of the normalizing integral) and τ_{rad} is the radiative lifetime. Since the latter is connected also to absorption cross sections, it is possible to calculate the emission cross section from the absorption cross section spectrum only, by using the following relation

$$\int \frac{\sigma_{em}(\lambda)}{\lambda} d\lambda = \frac{n_F}{n_A} \int_{S_0 \rightarrow S_1(abs)} \frac{\sigma_{abs}(\lambda)}{\lambda} d\lambda$$

Or

$$\sigma_{em}(\lambda) = \frac{n_F}{n_A} \frac{\lambda^4 f(\lambda)}{\int \lambda^3 f(\lambda) d\lambda} \int_{S_0 \rightarrow S_1(abs)} \frac{\sigma_{abs}(\lambda)}{\lambda} d\lambda$$

One should keep in mind the comments done in [Sect. 2.2.3](#) about the Strickler–Berg relation, regarding the integration boundaries. This last relation is particularly useful in practice as the absorption cross section spectrum, as explained in [Sect. 2.2.1.3](#), is easily measurable (Table 2.1).

2.2.5 Short and Long Wavelength Limits for Organic Lasers

In this section we try to answer the following question: while it seems relatively “easy” to chemically tune the absorption/emission spectrum of an organic system, why is it so difficult to synthesize a molecule or a light-emitting polymer emitting efficiently enough in the ultraviolet or in the infrared to make it a laser material? In practice indeed, unless using wavelength-conversion tricks [44, 45], organic solid-state lasers turn out to be mostly destined to serve in the visible range.

On the short-wavelength side, deep-blue or UV organic emitters are difficult to find, although they recently triggered a great interest in virtue of their applications in organic light-emitting diodes, especially phosphorescent emitters [46]. As explained above (see [Sect. 2.2.1.2](#)), UV emitters will in general be characterized by a short conjugation length. There is no simple connection between the size of a molecular conjugation segment and the quantum yield of fluorescence: for instance the theoretical quantum yields of fluorescence in the acene series does not vary in a simple way starting from naphthalene (two benzene rings stuck together, deep UV emission, quantum yield 31 %) to pentacene (five benzene rings, emission in the red, quantum yield 23 %) [47], and some UV dyes like coumarin 1 emitting around 380 nm have quantum yields as high as 0.85 in oxygen-free solutions for instance [48]. As far as organic lasing is concerned, the most relevant issue about UV emitters is more practical in nature and deals with photostability. As a laser effect in the UV requires excitation with photons of higher energy in the UV or the deep UV (although there has been a demonstration of 2-photon pumping of a blue

Table 2.1 Summary of the main photophysical parameters used to describe the physics of an organic laser medium. For each parameter, a typical value, a typical range and an example are given

Photophysical parameter	Typical value	Typical range	Examples (material, reference)
<i>Monomolecular (or intrachain) parameters</i>			
Absorption cross section σ_{abs} @ peak abs. wavelength (cm^2)	10^{-16}	10^{-17} – 10^{-15}	$2 \cdot 10^{-17}$ (MEH-PPV, [1]) $2.7 \cdot 10^{-16}$ (Pyromethene 567:copolymer P5MA-MMA, [29])
Fluorescence quantum yield Φ_f	70 %	0–100 %	30 % (MEH-PPV, [1]) 98 % (Coumarin 540:PMMA, [103])
Radiative lifetime τ_{rad} (ns)	5	1–10	1.62 (Neat film Horner-type MEH-PPV, [1])
Emission cross section σ_{em} @ peak em. wavelength (cm^2)	10^{-16}	10^{-18} – 10^{-15}	$2 \cdot 10^{-16}$ (Pyromethene 567:copolymer P5MA-MMA, [29]) $1.1 \cdot 10^{-16}$ (Horner-type MEH-PPV, [1])
Intersystem crossing rate k_{ISC} (s^{-1})	10^7	10^6 – 10^8 (10^{12a})	$6.7 \cdot 10^6$ (F8BT, [104])
Triplet state T_1 lifetime τ_T (s)	10^{-5}	10^{-3} – 10^{-7} s	$4 \cdot 10^{-6}$ s (MEH-PPV, [62])
Triplet-triplet $T_1 \rightarrow T_n$ absorption cross section σ_{TT} (cm^2)	10^{-16}	10^{-17} – 10^{-15}	$2 \cdot 10^{-16}$ (F8BT, [74])
<i>Binolecular (or interchain) parameters</i>			
Singlet-singlet annihilation rate k_{SS} (cm^3/s)	10^{-9}	10^{-11} – 10^{-7}	$2.6 \cdot 10^{-9}$ (F8BT, [105])
Singlet-triplet annihilation rate k_{ST} (cm^3/s)	10^{-9}	10^{-10} – 10^{-8}	$5.2 \cdot 10^{-10}$ (Polyfluorene, [106])
Triplet-triplet annihilation rate k_{TT} (cm^3/s)	10^{-12}	10^{-14} – 10^{-10}	10^{-14} (MEH-PPV, [107])
Singlet-polaron annihilation rate k_{SP} (cm^3/s)	10^{-9}	10^{-10} – 10^{-8}	$1.2 \cdot 10^{-8}$ (PPV, [108])
Triplet-Polaron annihilation rate k_{TP} (cm^3/s)	10^{-12}	10^{-13} – 10^{-12}	10^{-12} (DCM2:CBP, [66])

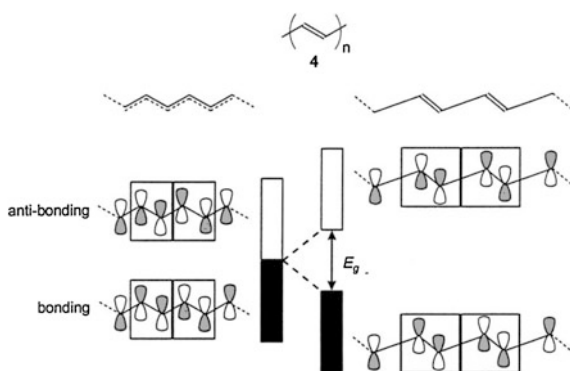
^a Values $\geq 10^{12} \text{ s}^{-1}$ for intersystem crossing rates only apply for phosphorescent emitters containing heavy metal atoms (platinum or iridium organo-metallic complexes) which induce a very strong spin-orbit coupling. However, up to now these materials have not proven to be useful for lasing

polyfluorene laser [49]), this causes extremely fast degradation of the molecule, as high-energy photons have enough energy to cause direct bond breaking with creation of reactive radicals. Because of the large potential interest for spectroscopy, substantial efforts have however been done to look for stable and efficient UV emitters. Silafluorenes [50] or spiro-compounds [51] are good candidates for this purpose: the lowest lasing wavelength achieved to date directly from an organic semiconductor film is 361.9 nm [52], obtained with a thermally-evaporated spiro-terphenyl film.

In the infrared side, the reasons why it is hard to obtain emission from organic systems above ~ 700 nm are different and related to both an emission and an absorption issue. First of all, the emission from low-bandgap materials is fundamentally restricted by the “energy gap law” [53], an empirical law stating that the nonradiative decay rate of an excited state increases exponentially as the energy gap decreases. Telecommunications, biomedical applications (for instance, deep-tissue imaging) and probably in a near future plasmonics, will however keep on motivating research towards efficient deep-red or infrared gain materials and lasers. There have been recent reports of lasing operation from 890 to 930 nm [54], or even at 970 nm with a commercial dye (LDS 950) doped in a fluorinated polyimide waveguide [55]. The evidence of stimulated emission was brought through gain measurements at a wavelength as high as $1.3\text{ }\mu\text{m}$ in IR1051 dye [56] with a measured gain of 11 cm^{-1} under 1064-nm pumping.

But if emission meets this fundamental limit, we may wonder what happens for absorption bands: can we build *pi*-systems with bandgaps as low as we want, provided that we allow more and more bonds to be shared along a *pi*-conjugated segment? The question is worth asking, because long chains are met in conjugated polymers, and because building low bandgap organic materials is of considerable practical interest, for organic electronics or photovoltaics for instance, where maximizing the absorption of the red part of the solar spectrum is a long-sought objective [57]. If we take the very simple example of *trans* polyacetylene (see Fig. 2.12), which goes logically upon examination after the case of the smaller butadiene molecule considered in Sect. 2.2.1.2, one should expect the following scenario: as more and more π orbitals are shared, the gap between the HOMO and

Fig. 2.12 Illustration of the “bond length alternation” principle in long *trans*-polyacetylene chains, and its consequences on the opening of a bandgap (Peierls instability). Courtesy of E.W. Meijer. Reprinted from [100] Copyright (2001), with permission from Elsevier



LUMO should decrease (see Fig. 2.6 for the case of oligothiophenes) until it eventually completely collapses to form a one-dimensional metal. This would indeed happen if the bond lengths between all carbon atoms were strictly identical and the electrons *fully* delocalized over the whole molecule; however this does not occur because this kind of equidistant linear chain structure happens to be unstable, an effect known as the *Peierls instability* [58]. The Peierls instability can be briefly understood as follows: consider that some extra energy is brought to the molecule which causes an elastic deformation, or a phonon, that results in alternating longer and shorter bonds; this excess of elastic energy stored by the molecule also produces a periodic potential for the *pi*-electrons. This periodic potential opens up a gap: this well-known fact (responsible for the electronic energy gap in crystals, for photonic gaps in photonic crystals, etc.) from Brillouin theory means that there are two wavefunctions of different energies which are associated with the same wavenumber: one wavefunction where maximal values (i.e. with maximum chance to find the electron at this place) stand between the longer bonds, and the other one having its maxima between the shorter bonds; of course the latter one has a lower energy since electrons are in average at shorter distance from the nuclei and are therefore more stabilized. It has been shown by Peierls [58] that the loss in the electronic energy of the molecule resulting from this gap opening is higher than the elastic energy required to generate it, meaning that the situation of “bond length alternation” is energetically favorable [59]. This is not systematically the case in all conjugated systems (in phenyl rings for instance the bond lengths are strictly equivalent), but here in the case of simple linear polyenic systems typically a gap of at least ~ 1.5 eV remains, which corresponds to a maximum wavelength for light absorption around 800 nm. This is the reason why it is generally difficult to find *pi*-conjugated polymers that are efficient in absorbing infrared radiation (and even worse in emitting IR beyond 1 μm). Synthetizing conjugated polymers with a low gap is useful for many purposes and is a hot topic of research: in the 80–90s it was more oriented towards the search for a zero-band-gap polymer capable of forming an intrinsically conductive material, namely a truly organic “synthetic metal” for energy storage or anti-static coatings [60]. Around the turn of the millennium, optoelectronics applications and organic photovoltaics became the driving forces of this research. However it must be noticed that as far as lasers are concerned, this lack of organic materials in the near IR is not problematic since it’s a region where inorganic semiconductors and crystals already densely occupy the room.

2.3 Triplet States and Their Influence on Lasing

Although triplet states are somewhat elusive (they are usually not luminescent), they play a crucial role in organic laser physics. The harvesting of triplet excitons in phosphorescent organic light emitting diodes has been a real breakthrough in this area [61], allowing for a fourfold increase of their quantum efficiency; since

then triplet states have been the subject of intense investigations in relation to the engineering of organic devices. As far as organic lasers are concerned, this starts from the understanding of the temporal dynamics in OSC lasers [41, 62, 63] and goes up to the development of advanced strategies for monitoring triplet decay, e.g. by adding to the active medium some “triplet scavengers” [64] or “triplet managers” [63], or through a clever use of metallic nanostructures acting as “plasmonic sinks” to remove the triplets [65]. Triplets also hold a central responsibility for the huge obstacles that stand on the road leading to the realization of an electrically-pumped organic laser diode [66–68]. For all these reasons triplets certainly deserve a particular attention in this chapter dedicated to the fundamentals of organic lasers. This chapter presents the basics of triplet states, but they will keep the top line in the next subsections dedicated to intermolecular phenomena and temporal dynamics of solid-state lasers. A comprehensive overview of triplet states in organic semiconductors can be found in the excellent review of Köhler and Bässler [69], from which many of the data presented in this section have been extracted.

2.3.1 Nature of Triplet States

A distinctive feature of organic semiconductors and more generally of all organic *pi*-conjugated systems used for lasing applications is the existence of well-defined spin states for the excited states. The spin of a state is given by the total spin of all electrons in all molecular orbitals; however electrons in filled orbitals are paired (one spin up, one spin down) so they contribute zero to the total spin. The spin is hence that of a two-electron system, one in the HOMO state and the other one in the LUMO state. The wavefunction describing the excited state can be written as a function of the two spatial coordinates \mathbf{r}_1 and \mathbf{r}_2 for each electron, and expressed as a product of a spatial wavefunction by a spin wavefunction:

$$\psi(r_1, r_2) = \psi_{\text{spatial}}(r_1, r_2)\psi_{\text{spin}}(r_1, r_2)$$

Two important principles of quantum mechanics have to be invoked here: first, the two electrons are indistinguishable, meaning that the probability density must verify $|\psi(r_1, r_2)|^2 = |\psi(r_2, r_1)|^2$. Secondly, the Fermi exclusion principle implies that the wavefunctions $\psi(r_1, r_2)$ and $\psi(r_2, r_1)$ cannot be the same, so they have to be of opposite signs $\psi(r_1, r_2) = -\psi(r_2, r_1)$ to be in accordance with the first relation: the total wavefunction has to be antisymmetric with respect to the exchange of the two electrons. This can be done in two ways: either $\psi_{\text{spatial}}(r_1, r_2)$ is symmetric and $\psi_{\text{spin}}(r_1, r_2)$ is antisymmetric, or the opposite. The wavefunctions of the four eigenstates of the two-particle system are summarized in Fig. 2.13. There is only one way to build an antisymmetric spin function for the two-electron system starting from linear combinations of one-electron spin states, this is the

Singlet state (total spin $S = 0$, $M_S = 0$):

symmetric spatial wavefunction, antisymmetric spin wavefunction

$$\psi_S(r_1, r_2) = \psi_{spatial}^{sym}(r_1, r_2) \frac{1}{\sqrt{2}} \{\uparrow_1 \downarrow_2 - \downarrow_1 \uparrow_2\}$$

Triplet states (total spin $S = 1$, $M_S = -1, 0$ and 1):

antisymmetric spatial wavefunction, symmetric spin wavefunction

$$\psi_T^1(r_1, r_2) = \psi_{spatial}^{antisym}(r_1, r_2) \frac{1}{\sqrt{2}} \{\uparrow_1 \downarrow_2 + \downarrow_1 \uparrow_2\}$$

$$\psi_T^2(r_1, r_2) = \psi_{spatial}^{antisym}(r_1, r_2) \{\uparrow_1 \uparrow_2\}$$

$$\psi_T^3(r_1, r_2) = \psi_{spatial}^{antisym}(r_1, r_2) \{\downarrow_1 \downarrow_2\}$$

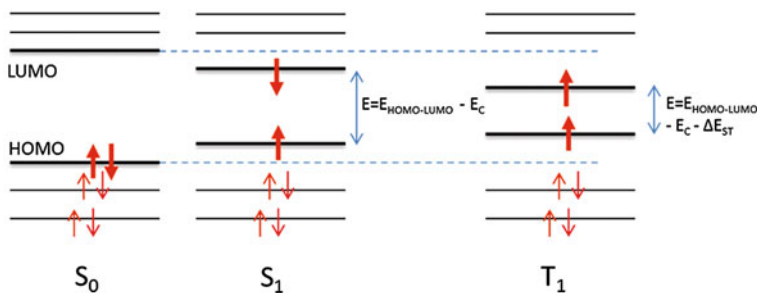


Fig. 2.13 Top singlet and triplet eigenstates wavefunctions. The \uparrow and \downarrow arrows denote the spin wavefunctions of the one-electron states with eigenvalues $s = 1/2$ and $m_s = 1/2$ and $s = 1/2$, $m_s = -1/2$ respectively. *Bottom* singlet and triplet states energy levels in an orbital configuration scheme. The S_1 and T_1 energy levels are shifted with respect to the HOMO–LUMO levels of the ground-state molecule by Coulomb and exchange interactions. The singlet state energy is given by $E_{S1} = E_{HOMO-LUMO} - J + K = E_{HOMO-LUMO} - E_c$, where $E_c = J(\text{coulomb integral}) - K(\text{exchange integral})$ is related to the exciton binding energy in an organic semiconductor; the Coulomb integral physically represents the coulomb attraction between the electron and hole in a pi-conjugated system. The triplet state energy is given by $E_{T1} = E_{HOMO-LUMO} - J - K = E_{HOMO-LUMO} - E_c - \Delta E_{ST}$, where $\Delta E_{ST} = 2K$ is the exchange energy. The exchange energy is an electrostatic term which reflects that the hole and the electron tend to be closer in a triplet state than in a singlet state because of the symmetry of the spatial part of the wavefunction (see text)

singlet state S_1 , necessarily associated to a symmetric spatial wavefunction. In contrast, there are three symmetric spin eigenfunctions with a total spin $S = 1$, these are the triplet states.

Under electrical excitation, these four states have equal probabilities to be formed upon recombination of two spin $1/2$ polarons (one hole and one electron), so the singlet formation yield is only 25 % in a fluorescent organic light-emitting diode.

2.3.2 The Exchange Energy

Triplet states lie lower in energy than singlet states by an amount ΔE_{ST} called the exchange energy or the singlet–triplet splitting (equal to twice the exchange integral K), whereas the three triplet states have the same energy³ [69].

The reason why triplet states have a lower energy than singlet states can be understood from a physically-intuitive argument exposed in [70] (p. 68) or in [16] (p. 26), from which we only extract here the key idea. We have already seen in Sect. 2.1.2.1 that in organic semiconductors, the exciton⁴ binding energy E_b caused the optical gap to be somewhat lower than the transport gap, which was itself lower than the HOMO–LUMO gap. Using a crude classical picture, this is because within the HOMO and LUMO bands the “free” hole and electron will seek the position where they are the more stabilized by their mutual attraction, making it more difficult to separate them into charges. The *exchange interaction* is responsible for the lowering of the triplet state energy and for the increase of the singlet state energy by the same amount K . Its nature is also purely electrostatic like the coulomb interaction [70], it is not a magnetic effect due to spin, but rather a pure quantum mechanical effect without classical analog which originates from the symmetry requirement of the spatial part of the wavefunctions. Indeed, for triplet states having an antisymmetrical spatial wavefunction, the two electrons can never be found at the same place because an antisymmetrical function $\psi_{\text{spatial}}(r_1, r_2)$ has necessarily a node for $r_1 = r_2$. Conversely, it is not forbidden for a singlet excited state with a symmetrical spatial wavefunction that electrons reside close to each other. With this crude picture in mind, we understand that electrons are more likely to be kept away from each other (or equivalently, for the hole and the electron to be kept closer to each other) in a triplet state than in a singlet state, hence leading to a triplet state having a lower potential energy.

From a quantum mechanical point of view, the exchange energy ΔE_{ST} scales exponentially with the overlap of the electron and hole wavefunctions [71]. Surprisingly, it was found to be around 0.7 eV in virtually all conjugated polymers, independently of the chemical structure, at the condition that the first excited state

³ There is a small energy difference between the three triplet substates because of their different m_s quantum numbers, called the Zero Field Splitting (because it exists even in absence of an applied magnetic field) due to spin–spin interactions, however it is very low (from a few μeV to a few meV in metal–ligand charge transfer complexes) and is hence only detectable at cryogenic temperatures.

⁴ The word *exciton* usually describes any *mobile* excited state, i.e. it is applicable whenever the excitation is able to travel or diffuse—to a nearby molecule for instance in the case of a molecular solid. The concept associated with the “exciton binding energy” is still valid for an oligomer or a dye dispersed in a non-conjugated matrix, although it may just be called the coulomb interaction in this case. Note also that the exciton binding energy in the case of an OSC carries more physical insight when it is defined with respect to the *transport gap*, as this becomes equal to the energy required to break the exciton into a pair of separated charges; in a dye-doped polymer the Coulomb energy can be expressed directly with respect to the HOMO–LUMO gap.

has a π - π^* character [69, 71]. In small molecules it may vary from ~ 0.1 to more than 1 eV. In Metal-to-Ligand Charge Transfer complexes for instance (mostly used in phosphorescent OLEDs), an electron is physically removed from the metal towards the ligand upon absorption of a photon, and this poor HOMO–LUMO overlap creates exchange energies as low as 0.2–0.3 eV [69]. In contrast, simple planar molecules like anthracene have an exchange energy as high as 1.5 eV [72]. The exchange energy is an important parameter as it is intimately connected with the Intersystem crossing rate (see below).

2.3.3 Optical Generation of Triplet States by Intersystem Crossing

The Wigner rule imposes that spin is conserved during an optical transition, meaning that only the S_1 state can be populated when a photon is absorbed from the ground state. This corresponds to a magnetic moment conservation rule, as the photon does not carry magnetic moment. However strict spin conservation during an optical transition would be true in a world where spin–orbit coupling does not exist. Spin–orbit coupling represents the magnetic mutual interaction between orbital momentum L and spin S : it is actually never zero (the spin–orbit coupling varies like Z^4 where Z is the atomic number), and it becomes especially strong when a heavy atom is present in the molecular structure [36, 73].

Spin–orbit interaction leads to a change in the selection rules, as L and S are not any more “good” quantum numbers to describe the system. It has two major consequences that are of interest for our subject: i) the T_1 - S_0 transition becomes slightly allowed, the triplet state acquires a finite lifetime τ_T , though the latter remains several orders of magnitude longer than the singlet lifetime, typically in the μ s to the ms range; and ii) a “spontaneous transfer” of the S_1 population towards the lower T_1 level becomes possible, called *intersystem crossing*, with a rate k_{ISC} defined by

$$\frac{dT_1}{dt} = k_{ISC}S_1$$

Intersystem crossing occurs because as the spin S is no longer a good quantum number, the spin states still referred to as “singlet” and “triplet” states are not in reality the true eigenstates of the system. For fluorescent emitters, ISC occurs within a typical timescale $1/k_{ISC}$ of the order of hundreds of ns ($k_{ISC} \sim 10^7 \text{s}^{-1}$). For phosphorescent emitters having a very strong ISC rate because of the presence of heavy atoms (Pt, Ir), the singlet state is not practically observable as any population in the singlet state very rapidly ends up in the triplet state with a timescale $1/k_{ISC} \sim \text{ps}$.

The magnitude of k_{ISC} depends on the strength of the spin–orbit coupling and on the vibrational overlap between the initial and final wavefunctions. It follows the energy gap law for nonradiative transitions, i.e. it can be written as

$$k_{ISC} \propto \exp(-A \Delta E)$$

where ΔE is the energy difference between the two states involved (and A is some constant). This means that high exchange energies are wanted to minimize intersystem crossing. This also means that the most efficient route for ISC will be first an horizontal transfer ($\Delta E = 0$) from the lowest vibrational state of S_1 towards a high-energy vibrational state of T_1 , followed by a rapid vertical Internal Conversion (multiphonon decay) down to the lowest vibrational state of T_1 , as sketched in Fig. 2.14, instead of a direct passage with $\Delta E = \Delta E_{ST}$. This picture of a horizontal transition followed by a very fast vertical decay is thought to be a correct general picture for nonradiative transitions between electronic states [69].

Even when no heavy atom is present in the molecule, some fluorescent dyes or polymers can have quite high intersystem crossing rates: the archetype for this is benzophenone, with $k_{ISC} = 10^{11} \text{ s}^{-1}$ where the torsion of phenyl rings enables an efficient mixing of electronic states having different angular momenta.

2.3.4 Triplet Absorption

Once a molecule is in the T_1 state, it can absorb a photon toward a higher-lying triplet state, and because the transition is spin allowed, cross sections are high and typically of the same order of magnitude as singlet–singlet transitions ($\sigma_{TT} \sim 10^{-16} \text{ cm}^2$). The first triplet state after T_1 that can be accessed optically is referred to as T_n , since the exact number of triplet states above is not usually known. Excitation to a T_n state will be generally followed by a fast nonradiative decay back to T_1 , but this recovery is not complete: for instance, recovery experiments in the polymer F8BT have shown that 80 % of the T_n states relax back to T_1 rapidly (within 300 fs), while the remaining 20 % are supposed to end up in electron–hole pairs [74].

Fig. 2.14 Intersystem crossing (ISC), Triplet Absorption (TA) and exchange energy (ΔE_{ST}) in a conjugated system

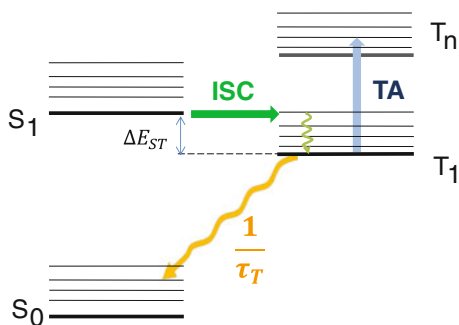
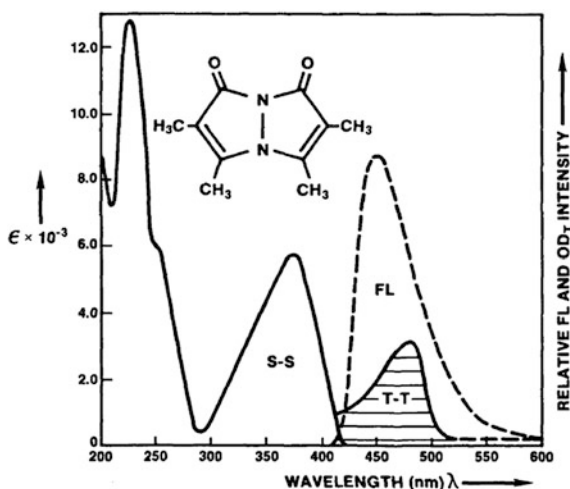


Fig. 2.15 Absorption (S-S), fluorescence (FL), and Triplet-Triplet (T-T) absorption spectrum of *syn*-(CH₃,CH₃)B in ethanol/ethyl ether 2:1 ratio. The T-T spectrum is recorded at 77 K. Reprinted with permission from [102]. Copyright 1986, American Institute of Physics



$T_1 \rightarrow T_n$ absorption bands are generally broad and significantly overlap with the fluorescence spectrum: it hence creates additional losses for the laser field that will be detrimental for efficiency, and will cause in the end the laser to shut down (see Sect. 2.5). In Fig. 2.15 is shown a typical Triplet-Triplet Absorption spectrum, evidencing the overlap between fluorescence (and hence gain) spectrum and T-T absorption.

There is a very intriguing fact about conjugated polymers with $\pi-\pi^*$ excited states (e.g. PPV derivatives or polyfluorenes): they happen to have a $T_1 \rightarrow T_n$ energy located around 1.5 eV, independently of the chemical structure. Because we already pointed out that the exchange energy was also similar, this means that a useful rule of thumb proposed by Köhler and Bässler [69] is to say that the T_1 state is 0.7 eV below the S_1 state, while the T_n state is 0.7 eV above the S_1 state for any conjugated polymer.

2.3.5 Phosphorescence: Are Triplet Emitters Suitable for Lasing?

Phosphorescence is the term used to describe luminescence from the triplet state T_1 : while it can be present in any molecule at low temperatures, it becomes exploitable in a device when a very strong spin-orbit coupling is introduced by the presence of a heavy atom in the structure. Considerable efforts have hence been devoted in the first decade of the millennium to develop efficient phosphorescent emitters for Organic Light-emitting diodes, based on Metal-to-Ligand Charge Transfer complexes of Platinum or Iridium. The motivation for this research was driven by the fact that, under electrical excitation, the four possible exciton states resulting from the recombination of two spin-1/2 polarons of random spin (up or

down) are created with equal probabilities, meaning that 75 % of triplets are formed, which are usually lost in fluorescent emitters. As the singlets end up very rapidly as triplets by ISC, electroluminescent devices based on phosphorescent emitters can reach 100 % internal quantum efficiency [75]. Good phosphorescent emitters must exhibit a very strong spin–orbit coupling to see their $T_1 \rightarrow S_0$ transition becoming frankly allowed. Green emitters are the most likely to be very efficient, since red emitters suffer from competition with nonradiative decay (it’s the energy-gap law), and since blue emitters, associated to singlet states lying in the UV because of the exchange energy, suffer from very problematic photostability issues.

Are phosphorescent emitters suitable for lasing? Building a population inversion between the T_1 state and a high-lying vibrational level of the S_0 level is not difficult. However, considering a T_1 excited state, stimulated emission $T_1 \rightarrow S_0$ with rate $\sigma_{em(T_1 \rightarrow S_0)} I T_1$ directly competes with $T_1 \rightarrow T_n$ absorption with rate $\sigma_{TT(T_1 \rightarrow T_n)} I T_1$, so that lasing in an otherwise lossless medium will be possible at a wavelength λ at the simple condition that the stimulated emission cross section exceeds the absorption cross section at this wavelength:

$$\sigma_{em(T_1 \rightarrow S_0)}(\lambda) > \sigma_{TT(T_1 \rightarrow T_n)}(\lambda) \quad (\text{condition of phosphorescent lasing})$$

This is a hard-to-meet requirement, because $T_1 \rightarrow S_0$ remains a forbidden transition in nature while $T_1 \rightarrow T_n$ is allowed, meaning that there is typically a three-orders-of-magnitude difference between the two cross sections, and unfortunately the two bands spectrally overlap significantly. A phosphorescent organic laser would be feasible if one is able to find a material where spin–orbit coupling is very strong, combined with a phosphorescence emission spectrum well shifted from the triplet absorption spectrum. Such a laser would be interesting since it would not experience the pulse duration limit encountered with singlet emitters, opening the way for a true CW laser. Accordingly, as triplets represent a huge obstacle in the route towards electrically-driven organic semiconductor lasers because they quench singlets or reabsorb the emitted laser light, achieving phosphorescent lasing would be an interesting achievement in this context too. Some attempts to observe Amplified Spontaneous Emission in highly-efficient phosphorescent emitters Ir(ppy)₃ [60] or Btp2Ir(acac) [76] have been tried without success.

2.4 Intermolecular Phenomena: Quenching and Energy Transfer

A chromophore in a solid-state material is never alone. It is surrounded by a large assembly of identical chromophores and by foreign elements (chromophores of a different kind, dissolved oxygen or water or any other impurities, metallic electrodes, etc.) which all may interact with it and *quench* the emission of the chromophore.

Quenching is a very general term designating the different mechanisms through which a singlet or a triplet state loses its excitation upon interaction with a foreign “quencher”. For light-emitting devices and particularly for lasers, quenching of emissive singlets is detrimental, whereas it may be conversely useful to quench the triplets as their accumulation causes absorption of the laser light.

Here we use the term “quenching” in its widest sense, as a loss of the excitation energy for a given emitter. This energy can be eventually lost as heat directly (the molecule switches to its own triplet state upon the influence of the quencher for instance), or transferred to another compound, where the energy may be transformed into heat as well, or into light if the acceptor is a chromophore. This is called *energy transfer*.

We will investigate the following phenomena:

- exciton diffusion and homo-FRET (Fluorescence Resonant Energy Transfer), which involve energy transfer from an excited fluorophore D^* to a fluorophore D of the same kind *in the ground state*;
- Singlet–singlet annihilation, singlet–triplet annihilation or triplet–triplet annihilation (SSA, STA, TTA), involving two fluorophores of the same kind *both in the excited state* D^* ;
- energy transfers between a donor D and an acceptor A of different kinds. If A is a light-emitting unit, then we form a host/guest system, in which D absorbs light, transfers the excitation to A , which finally emits the light. Host/guest systems form a widely used class of materials useful for laser action (Table 2.2).

2.4.1 Physical Origin of Quenching/Energy Transfer

Let D be a “donor” chromophore. Let’s examine how it may lose its energy by quenching. The rate equation for the excited state density (let’s note it D^* here) will be $\frac{dD^*}{dt} = -kD^*$. The transfer rate constant k depends on the distance r between D and the quencher (or acceptor) in two very different ways, which enable defining two types of mechanisms for quenching:

- (a) **“Long-range” quenching/Resonant Energy Transfer RET** (or FRET for Fluorescence Energy Transfer or Förster Resonant Energy Transfer).

It is a nonradiative dipole–dipole interaction, which does not however proceed through the emission and absorption of a photon (Fig. 2.16). The transfer rate constant k_{RET} can be expressed as:

Table 2.2 Summary of some bimolecular processes in organic materials (see text for details)

Excited molecule	Other element						Process
D^*	+	D	\rightarrow	D	+	D^*	Diffusion
D^*	+	D^*	\rightarrow	D	+	D^*	SSA/TTA
D^*	+	Q	\rightarrow	D			Quenching
D^*	+	A	\rightarrow	D	+	A^*	FRET

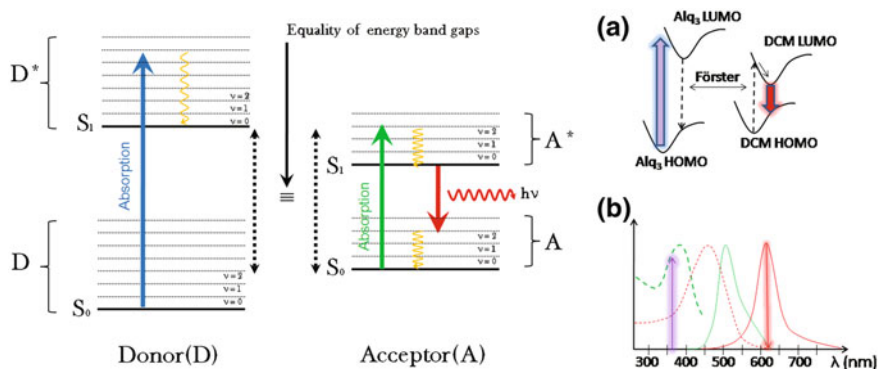


Fig. 2.16 Schematic representation of Förster resonant energy transfer (FRET). *Right (a)* Illustration of the host–guest Förster energy transfer between Alq₃ and DCM and *(b)* corresponding absorption (dashed line) and emission (full line) spectra. The Alq₃ host absorbs a UV pump photon and transfers its excitation through nonradiative dipole–dipole interaction to the guest; Förster energy transfer is efficient if the overlap between the emission spectrum of the host and the absorption spectrum of the guest is large. It results in a photon emission by the guest at a wavelength where the host absorption is almost zero, thus minimizing reabsorption losses

$$k_{RET} = \frac{1}{\tau_D} \cdot \left(\frac{R_0}{r} \right)^6$$

where τ_D is the donor lifetime (when no energy transfer occurs, \sim ns), and R_0 is the Förster radius, defined as the distance for which spontaneous decay of the donor and energy transfer to the acceptor are equally probable. FRET is only possible between dipole-allowed transitions (S–S or T–T for instance but not S–T) and is efficient if the overlap between the emission spectrum of the donor and the absorption spectrum of the acceptor is high enough.

The Förster radius R_0 is typically a few nanometers, that is several times the size of a molecular unit: FRET is a distance interaction. It can be calculated from the following relation [77]:

$$R_0^6 = \frac{9000(\ln 10)\kappa^2\Phi_D}{128\pi^5\mathcal{N}_A n^4} \int_0^\infty I_D(\lambda) \varepsilon_A(\lambda) \lambda^4 d\lambda$$

where Φ_D is the donor fluorescence quantum yield (when no transfer occurs), n is the average refractive index in the overlap spectral range, $I_D(\lambda)$ is the fluorescence spectrum of the donor (normalized so that the integral of I_D over λ is equal to unity), $\varepsilon_A(\lambda)$ is the acceptor molar absorption coefficient (in $\text{L mol}^{-1} \text{cm}^{-1}$), N_A is the Avogadro number and κ is an orientation factor (with κ^2 equal to 0.66 for free rotating molecules—in a liquid for example—and κ^2 equal to 0.476 for randomly dispersed acceptor molecules in a rigid medium—both in terms of relative distance and orientation).

The efficiency ρ of the energy transfer (or probability for D to transfer its excitation to A rather than decaying spontaneously) can be written as:

$$\rho = \frac{1}{1 + \left(\frac{r}{R_0}\right)^6}$$

The transfer efficiency is by definition equal to 50 % for $r = R_0$, and varies as $1/r^6$. A plethora bibliography can be found about FRET as it is a widely used technique in biochemistry and spectroscopy [78].

(b) Short-Range Quenching

For this type of interaction, a physical contact between the donor molecule (the quenched unit) D and the quencher Q must exist, i.e. the electronic clouds must overlap. As the electron density decreases exponentially with distance from the nuclei, the rate of quenching depends on the distance as:

$$k_Q = A \cdot \exp[-\beta(r - r_c)]$$

where r is the distance between the donor and the quencher, r_c is the distance of closest approach at molecular contact, A is a constant ($\sim 10^{13} \text{ s}^{-1}$) and β is typically $\sim 1 \text{ \AA}^{-1}$ [77].

There are at least three mechanisms for short-range quenching:

- **Intersystem crossing:** quenching of an excited state by molecular oxygen for instance is thought to occur by ISC: when O_2 comes in contact with a molecular unit, it accelerates its transfer to the triplet state where it becomes non-emissive [79].
- **Photoinduced Charge Transfer:** an electron (or a hole) is physically removed from the donor D towards the acceptor A to form a ($\text{D}^+ \text{A}^-$) complex: this kind of quenching is a highly-wanted phenomenon in organic solar cells for instance, where it has to be more efficient than fluorescence of the absorbing material, which is in this case an unwanted recombination phenomenon.
- **Dexter electron-exchange interaction (or Dexter energy transfer):** in this process, an electron is exchanged from the LUMO of the donor to the LUMO of the acceptor, while simultaneously a hole is exchanged from the HOMO of the acceptor to the HOMO of the donor. The net result is a transfer of the exciton. Compared to Förster RET, Dexter energy transfer also requires a spectral overlap of the emission spectrum of the donor with the absorption spectrum of the acceptor, but in contrast D and A must be “in contact”, and Dexter interaction does *not* require the transition to be dipole-allowed (hence Dexter transfer to/from triplet states is possible).

A summary of Förster versus Dexter interactions is presented in Fig. 2.17.

Up to now, to discuss the photophysics relevant for organic laser science, we did not pay much attention to differentiate neat organic solids (conjugated polymer

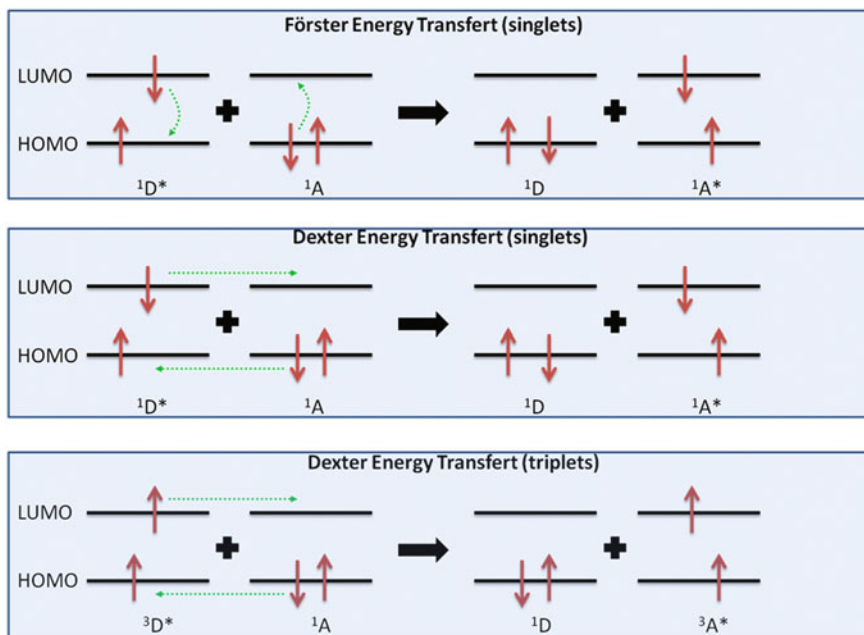


Fig. 2.17 Illustration of Förster energy transfer (*up*): it's a dipole–dipole interaction, formally equivalent to a photon emission by D which is reabsorbed by A (however no real photon is emitted); it does not require a contact between D and A, but an overlap between the D emission spectrum and the A absorption spectrum; furthermore the transition must be dipole-allowed, so that only singlet states can be concerned. For Dexter energy transfer, on the contrary, D and A electron clouds must overlap so that an simultaneous exchange of electrons and holes can occur. There is no restriction on selection rules and both triplets and singlets can intervene

films, molecular solids, molecular crystals) from dispersed emitters (dye-doped polymers). Now it is useful to remember that in a dispersed medium, only long range Förster RET is expected to occur between the active species (this may concern Singlet–singlet annihilation, singlet–triplet Annihilation, energy transfer to a ground state neighbor), to which one may add contact-type interactions but only with impurities or oxygen. Conversely, annihilation phenomena like Triplet–Triplet annihilation, or exciton diffusion are important in organic semiconductors but do not intervene in dispersed media.

2.4.2 Different Mechanisms of Bimolecular Interactions

Let's suppose we have a singlet excited state in a solid-state environment, that we shall note here D^* , because upon quenching it will donate its excitation and act as a donor. Several scenarii are possible, listed in the introduction. We here focus on

diffusion (and homoFRET), Singlet–Singlet annihilation (SSA), Singlet–Triplet annihilation (STA), and Triplet–Triplet annihilation (TTA).

2.4.2.1 Exciton Diffusion and HOMO-FRET

D^* can be quenched by another identical molecule or emissive unit D in the ground state. The process is then called diffusion:

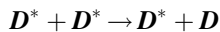


The transfer can proceed through a Dexter exchange interaction in neat films of OSCs, but may also arise when the two sites are away from each other, by FRET which is called in this case *homo-FRET* (only for singlets; the latter is efficient when there is a good overlap between absorption and emission spectrum, that is for a low Stokes shift). Diffusion is not directly a quenching loss mechanism, as the energy is just translated elsewhere, but it enhances the risk that the mobile excitation ends up in meeting a “real” killing quenching site. Exciton diffusion occurs within a typical exciton diffusion length $L_D \sim \sqrt{D\tau}$ where D is the diffusion constant and τ the exciton lifetime. Because triplets have lifetimes that are higher than singlet lifetimes, a typical order of magnitude for singlet diffusion length is a few nm, while for triplets it can reach several tens of nm or more [80, 81].

Homo-FRET is a non-negligible phenomenon in dispersed dye-doped polymer media even at low concentrations. Indeed, an active gain medium consisting of 1 % (in mass) of Rhodamine 640 molecules dispersed in a solid-state matrix of PMMA corresponds to a distance between adjacent molecules which is of the order of 3.3 nm if we assume a homogeneous blend, while the value of R_0 for the system {Donor = Acceptor = Rhodamine 640} is as high as 4.8 nm, because of a small Stokes shift for this molecule. As a consequence, the transfer efficiency in this case reaches 90 %. It falls at 50 % for a doping level of 0.4 % and is above 98 % for doping level higher than 2 %. HomoFRET can be evidenced by the depolarization of the fluorescence emission while increasing doping ratio [82].

2.4.2.2 Singlet–Singlet Annihilation

D^* can be quenched by another identical molecule or emissive unit D^* in the excited state:

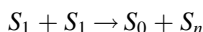


SSA is a process happening between two molecules in the first excited singlet state, i.e. when $D^* = S_1$. During this phenomenon the energy from one of the excited molecules is transferred to the second one. As a result, the first molecule falls back to its ground state and the second molecule gets promoted to a higher

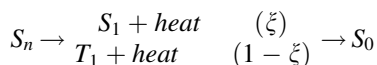
excited singlet state S_n which then relaxes either to the first excited singlet state S_1 with a probability ξ or to the triplet state T_1 with a probability $1 - \xi$.

Considering a probability ξ is a way to include intersystem crossing in the system in some way, and is consistent with the choice of some authors to treat ISC with a “yield” instead of a “rate”, as we see in detail in Sect. 2.5.2.2. While some authors [83] do not take this effect into account and assume that all S_n states end up as S_1 ($\xi = 1$), some others [62, 84] assume that ξ is 0.25, which means that an excited singlet state produces on average one singlet for three triplets, exactly in the same proportions as when two polarons (one hole and one electron) encounter to make an exciton in an electrically-driven device [85].

For SSA [83] the reaction is sketched on Fig. 2.18 and writes:



Followed by



The equation for the evolution of the S_1 population accounts for the fact that two singlets are lost, and only a fraction ξ of one of them is recovered, which writes:

$$\frac{dS_1}{dt} = -(2 - \xi)k_{SS}S_1^2$$

k_{SS} is of the order of $10^{-9} \text{ cm}^3/\text{s}$ (see Table 2.1) SSA is one of the only quenching phenomena that can explain the phenomenon of *concentration quenching* in dye-doped dispersed polymeric media, as it can arise through a long-range FRET mechanism provided that $S_0 \rightarrow S_1$ and $S_1 \rightarrow S_n$ bands spectrally overlap.

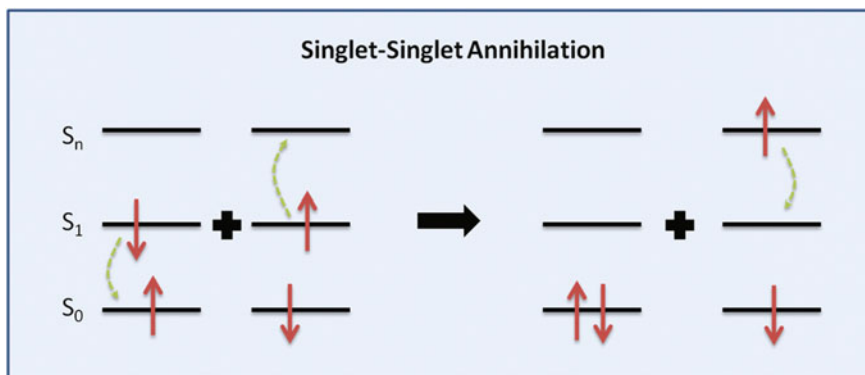
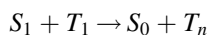


Fig. 2.18 Schematic representation of Singlet–Singlet Annihilation. Energy is transferred from one excited chromophore to a second excited chromophore resulting in a de-excitation of the first one along with excitation of the second chromophore to a higher excited state, from which it relaxes to the lowest excited state through fast non-radiative decay

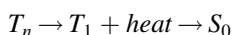
Concentration quenching causes the quantum efficiency to drop dramatically for dye mass ratios inside the polymer above only a few percents [83].

2.4.2.3 Singlet–Triplet Annihilation

STA is a process where a molecule in the first excited singlet state S_1 is quenched by another molecule in the excited triplet state T_1 in its vicinity. As a result, the latter is getting excited to a higher triplet state while the former relaxes to its ground state. The molecule that is raised to an upper excited triplet state will then go down to the first excited triplet state which eventually relaxes to the ground state.



Followed by



Here all excited-state triplets end up in the T_1 state, as reverse ISC is a very unlikely phenomenon. The rate equation for STA is then:

$$\frac{dS_1}{dt} = -k_{ST}S_1T_1$$

k_{ST} is of the order of $10^{-9} \text{ cm}^3/\text{s}$ (see Table 2.1). The simultaneous transitions $S_1 \rightarrow S_0$ and $T_1 \rightarrow T_n$ are both allowed meaning that STA can arise through a Förster-type reaction. List et al. have shown that FRET is indeed the dominant mechanism for STA in conjugated polymers [86].

2.4.2.4 Triplet–Triplet Annihilation

TTA has been the subject of many investigations and debates [69]. It plays a major role in the triplet dynamics in OSCs and especially for devices under electrical excitation, because triplets are abundant (75 % of excitons created by electron/hole pairs recombinations) and long-lived, so that their mutual destruction by TTA

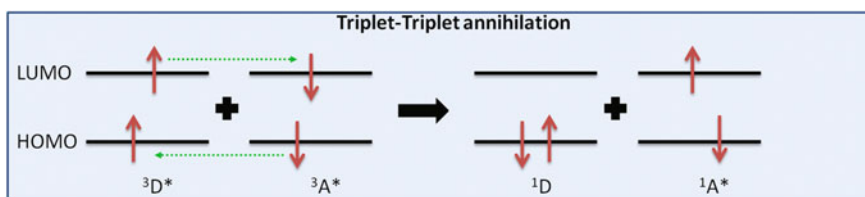
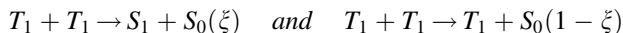


Fig. 2.19 Illustration of Triplet–Triplet annihilation (here occurring through a Dexter or exchange mechanism)

turns out to be an important issue. In the context of organic lasers under optical excitation, it is somewhat less important, and can be considered as a positive quenching phenomenon, as it helps depleting the triplet population and creating singlets out of triplets. TTA is incorporated in some organic lasers models [62, 84] (Fig. 2.19).

Because T-S transition are spin-forbidden, TTA can only be explained by a Dexter or exchange interaction, and simple images such as the one displayed in Fig. 2.18 for SSA fail at explaining what happens in a simple way [87]. TTA reaction can be written as [84]:



which is (at least formally) equivalent to two T_1 states reacting towards a high-lying S_n singlet state, which afterwards decays either towards S_1 with a probability ξ or towards T_1 with a probability $1 - \xi$, in a similar way as ξ was defined for SSA (see Sect. 2.4.2.2). The formation of singlet excitons S_1 from the annihilation of two long-lived triplet states is demonstrated experimentally through the observation of delayed luminescence. The rate equation for T_1 in presence of TTA is

$$\frac{dT_1}{dt} = [-2 + (1 - \xi)]k_{TT}T_1^2 = -(1 + \xi)k_{TT}T_1^2$$

k_{TT} is of the order of $10^{-12} \text{ cm}^3/\text{s}$ (see Table 2.1).

2.5 Equations for Organic Solid-State Lasers

In this section we derive a few simple equations that can serve as a basis for theoretical work with organic lasers. Triplets hold the key role here, because the piling up of these long-lived states hinders lasing in the CW regime.

Organic lasers can hence only emit *short pulses*, unless specific action is taken to avoid the triplet problem. A simple solution was found with liquid dye lasers which can run in CW mode because the continuous circulation of the fluid allows refreshing the medium permanently. Another option is to reduce the triplet lifetime by adding “triplet quenchers”, that is molecules that will interact preferentially with triplets to bring them back to the S_0 state through internal conversion.

2.5.1 An Equation for the Evolution of the Photon Density

Let’s first write the equation governing the evolution of photon density q (in m^{-3}) at time t in the laser mode. In this discussion we assume a single-mode laser. Photons can be created by spontaneous or stimulated emission, but also reabsorbed or coupled out of the cavity to build up the useful laser light beam. This writes:

$$\frac{dq}{dt} = \left(\frac{dq}{dt}\right)_{stim} + \left(\frac{dq}{dt}\right)_{spont} + \left(\frac{dq}{dt}\right)_{material\ losses} - \frac{q}{\tau_{cav}}$$

The photon density has two feeding terms, spontaneous and stimulated emission, and two loss terms; The losses are of two different natures: the losses due to the material intrinsic photophysics (reabsorption of laser light, triplet–triplet absorption), referred here to as *material losses*, and the losses due to the cavity. The latter are the outcoupling losses of the mirrors, for an external cavity, or the losses embedded in the laser resonator, e.g. scattering or diffraction losses for a Distributed Feedback laser, for instance. Cavity losses can be written as $-\frac{q}{\tau_{cav}}$ where τ_{cav} is the *photon lifetime in the cavity*. The cavity lifetime physically represents the dwelling time of a photon injected into an optical cavity before it comes out. It will be of course high when long cavities with high reflectivity mirrors are used. In the case of a simple linear cavity of length L with two mirrors of reflectivities R_1 and R_2 facing one in front of each other enclosing a medium with a single-pass absorption A ($0 < A < 1$), it is found to be [88]:

$$\tau_{cav} = \frac{-2L}{c \ln [R_1 R_2 (1 - A)^2]}$$

The term $\left(\frac{dq}{dt}\right)_{stim}$ accounts for stimulated emission (as well as for reabsorption from the laser transition lower level, but since the latter is quickly depopulated towards the ground state, this reabsorption is usually neglected) and writes:

$$\left(\frac{dq}{dt}\right)_{stim} = \Gamma \sigma_{em} I \Delta N = \Gamma \sigma_{em} \frac{c}{n_{eff}} q S_1$$

where the intracavity laser intensity I relates to q through $I = \frac{c}{n_{eff}} q$ (n_{eff} is the effective refractive index of the laser mode), ΔN is the population inversion density, equal to the S_1 singlet state population density.

Γ is the confinement factor defined by

$$\Gamma = \frac{\int_{active\ layer} |\langle \Pi(x) \rangle| dx}{\int_{-\infty}^{\infty} |\langle \Pi(x) \rangle| dx}$$

where $\langle \Pi(x) \rangle$ is the time-averaged Poynting vector (the power flow of the optical wave) in a gain medium consisting of an active layer confining light in the x -direction, and otherwise infinite in y - and z - directions (see Fig. 2.20). For external cavities or vertical geometries, the confinement factor is equal to $\Gamma = \frac{\text{volume of the active medium}}{\text{laser mode volume}}$; it can be well below unity and is in this case given by the ratio d/L of the gain medium thickness over the cavity length.

The term $\left(\frac{dq}{dt}\right)_{spont}$ accounts for spontaneous emission: it is the “feeding term” or the “trigger” in this equation which will provoke the avalanche of photons through the stimulated emission process. Although spontaneous emission

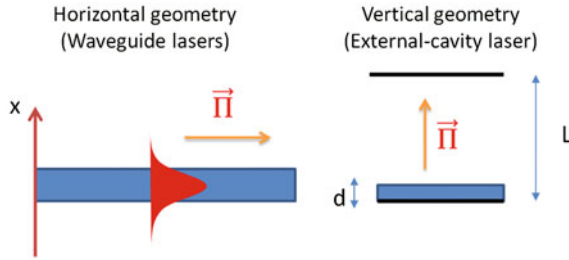


Fig. 2.20 Definition of the confinement factor: $\frac{\int_{\text{active layer}} |\langle \Pi(x) \rangle| dx}{\int_{-\infty}^{\infty} |\langle \Pi(x) \rangle| dx}$ where $\langle \Pi(x) \rangle$ is the time – average Poynting vector. In a horizontal geometry the light propagation direction (or the Poynting vector $\vec{\Pi}$ representing the power flow of the optical wave) is orthogonal to the confining direction x of the waveguide; the confinement factor is hence close to 1. In a vertical geometry with an external mirror (VECSOL case) the Poynting vector is along the thin-film direction and is just equal here to $\sim d/L < 1$

contributes generally in a negligible way to the photon density in the laser mode while the laser is operating, it is essential to give to this term a correct value to start the process. However, mistaking about this term is not dramatically important, except maybe if we are interested in laser behavior near threshold or lasers operating below the saturation intensity.

Many authors [62, 65, 67, 89] chose to write this term as $\left(\frac{dq}{dt}\right)_{\text{spont}} = \Gamma \beta_{\text{spont}} \frac{S_1}{\tau_F}$ where β_{spont} represents the fraction of all spontaneous photons (produced at a rate $\Gamma \frac{S_1}{\tau_F}$) emitted in the mode volume. In the reports cited above and quite generally in the literature, following [90] β_{spont} is taken equal to $\sim 10^{-4}$; however this term depends on the specific geometry of the laser resonator, and can become significantly higher in micro or nanocavities where only few optical modes are supported. In the general case, we may use the following result [91]: “the spontaneous emission rate into one mode is equal to the rate of stimulated emission induced by one photon in this particular mode”. Let I_1 be the intensity of one photon in a mode volume V_{mode} , then $I_1 = \frac{c}{V_{\text{mode}}}$, and

$$\left(\frac{dq}{dt}\right)_{\text{spont}} = \Gamma \sigma_{em} I_1 \Delta N = \Gamma \sigma_{em} \frac{c}{V_{\text{mode}}} S_1$$

Then we obtain this simple relation for β_{spont} : $\beta_{\text{spont}} = \sigma_{em} I_1 \tau_F$.

At last, the term $\left(\frac{dq}{dt}\right)_{\text{material losses}}$ accounts for ground-state reabsorption at the laser wavelength, excited-state absorption ($S_1 \rightarrow S_n$) and Triplet–Triplet absorption (and other relevant terms if any, depending on the specific nature of the system).

$$\begin{aligned}
 \left(\frac{dq}{dt}\right)_{\text{material losses}} &= -\sigma_{abs}^{S_0 \rightarrow S_1}(\lambda_{laser})S_0I - \sigma_{abs}^{S_1 \rightarrow S_n}(\lambda_{laser})S_1I - \sigma_{abs}^{T_1 \rightarrow T_n}(\lambda_{laser})T_1I \\
 &= -\alpha_{reabs}I = -\alpha_{reabs}\frac{c}{n_{eff}}q
 \end{aligned}$$

In conclusion, we have this final formula governing the evolution of the intracavity photon density:

$$\frac{dq}{dt} = \left[\Gamma\sigma_{em}S_1 - \alpha_{reabs} - \frac{n_{eff}}{c\tau_{cav}} \right] \frac{c}{n_{eff}}q + \Gamma\sigma_{em}\frac{c}{V_{mode}}S_1$$

This equation couples the photon density q to the population inversion S_1 .

Rate equations will give us the missing relations in order to solve completely the problem.

2.5.2 Rate Equations: A Set of Equations Governing the Flow between Different States

Organic lasers are properly described by *rate equations* governing how the populations in the different states flow from a state to another under the effects of absorption, spontaneous emission, stimulated emission or nonradiative decays (internal conversion and intersystem crossing). However taking into account every vibrational level, or even every electronic level susceptible to intervene in the laser process is an impossible and irrelevant task. Equations are not more complicated when many higher excited states are involved to account for excited-state absorption or bleaching for instance, and models incorporating as many states as wanted can be easily implemented and solved numerically (even though a complex model with many unknown parameters will of course not be very helpful in capturing the physics of a given device).

Rate equations can be as complex as desired, if all quenching effects and absorption/emission to higher-lying excited states are considered. Incorporating all bimolecular phenomena (SSA, TSA, TTA) discussed in [Sect. 2.4.2](#) as well as ISC enable writing for S_1 and T_1 the following set of equations:

$$\begin{cases}
 \frac{dS_1}{dt} = \sigma_{abs}I_pS_0 - \left(\frac{1}{\tau_F} + \sigma_{em}I\right)S_1 - k_{ST}S_1T_1 - (2 - \xi)k_{SS}S_1^2 - k_{ISC}S_1 \\
 \frac{dS_0}{dt} = -\sigma_{abs}I_pS_0 + \left(\frac{1}{\tau_F} + \sigma_{em}I\right)S_1 + k_{ST}S_1T_1 + \frac{T_1}{\tau_T} + k_{SS}S_1^2 + (1 + \xi)k_{TT}T_1^2 \\
 \frac{dT_1}{dt} = k_{ISC}S_1 - \frac{T_1}{\tau_T} + (1 - \xi)k_{SS}S_1^2 - (1 + \xi)k_{TT}T_1^2
 \end{cases}$$

Here S_1 , T_1 and S_0 are the normalized densities ($S_1 + T_1 + S_0 = 1$); σ_{abs} , σ_{em} are the absorption/emission cross sections (m^2) resp. at the pump/laser wavelength, I_p and I are resp. the pump and the intracavity laser intensity expressed in photonic units ($\text{photons}/\text{m}^2/\text{s}$); τ_F and τ_T are the fluorescence (singlet) lifetime and the triplet lifetime, respectively.

Here we also incorporated the equation for S_0 , following the assumption that $S_1 + S_0 + T_1 = 1$. This assumption neglects all sources of permanent photodegradation (the total number of molecules is constant), and is essentially useful at high pumping intensities when the ground state can be depleted. Most of literature reports make a stronger approximation, assuming that only low inversions are obtained, i.e. $S_1, T_1 \ll 1$ (which is certainly true in OSCs but is questionable in dispersed media where the chromophore density is low and absorption saturation regime may be attained); this means that S_0 is taken as a constant equal to 1, and the pumping term hence becomes described by a *constant pump rate* $G = \sigma_{abs} I_p$ (s^{-1}). With this assumption, and using the photon density $\frac{n_{eff}}{c} I = q$ instead of the intracavity intensity, we have the following set of equations [62, 67, 92]:

$$\begin{cases} \frac{dS_1}{dt} = G - \left(\frac{1}{\tau_F} + \sigma_{em} \frac{c}{n_{eff}} q \right) S_1 - k_{ST} S_1 T_1 - (2 - \xi) k_{SS} S_1^2 - k_{ISC} S_1 \\ \frac{dT_1}{dt} = k_{ISC} S_1 - \frac{T_1}{\tau_T} + (1 - \xi) k_{SS} S_1^2 - (1 + \xi) k_{TT} T_1^2 \end{cases}$$

2.5.2.1 The 4-Level Approximation

In absence of quenching (i.e. STA, SSA, TTA, etc.) and if we totally neglect the influence of triplet states, the laser acts as a four-level system. This is a relevant approximation in experimental conditions where *pulsed sources with durations much smaller than the ISC time constant (on the order of hundreds of ns) are used*. Triplet accumulation and the subsequent phenomena are hence negligible. In addition, emission reabsorption from S_1 to a higher excited singlet state and stimulated emission at the pump wavelength are also neglected. The equations then simply write:

$$\begin{cases} \frac{dS_1}{dt} = \sigma_{abs} I_p S_0 - \left(\frac{1}{\tau_F} + \sigma_{em} I \right) S_1 \\ \frac{dS_0}{dt} = -\sigma_{abs} I_p S_0 + \left(\frac{1}{\tau_F} + \sigma_{em} I \right) S_1 \end{cases}$$

where I_p is the pump intensity, I the intracavity laser intensity, expressed in photonic units.

2.5.2.2 Taking Triplet States Into Account: The “Constant Yield” Versus “Constant Rate” Models

The 4-level model can be useful for many purposes but fails at capturing most of the interesting physics with organic materials which rely on the existence of triplet states or bimolecular interactions. Triplet filling is a well-known effect which generally hinders lasers from operating in the CW regime.

There has been intense research to determine how triplet states are formed under optical as well as electrical excitation [69, 93], and triplets have become extremely studied with the advent of triplet-harvesting phosphorescent organic light-emitting diodes [61].

The most widespread picture, used for decades in liquid dye lasers, consists in assuming that all triplets are created through intersystem crossing from the first singlet excited state S_1 with an intersystem crossing rate k_{ISC} (s^{-1}). The rate equations in a “constant triplet formation rate” or “ k_{ISC} model” write:

$$\begin{cases} \frac{dS_1}{dt} = \sigma_{abs} I_p S_0 - \left(\frac{1}{\tau_F} + \sigma_{em} I + k_{ISC} \right) S_1 \\ \frac{dS_0}{dt} = -\sigma_{abs} I_p S_0 + \left(\frac{1}{\tau_F} + \sigma_{em} I \right) S_1 + \frac{T_1}{\tau_T} \\ \frac{dT_1}{dt} = k_{ISC} S_1 - \frac{T_1}{\tau_T} \end{cases}$$

The constant rate model has been used for most works on solid-state dye-doped polymers or liquid dye lasers [16, 94, 95] and also in many recent works devoted to the dynamics of organic semiconductor films under optical excitation [62, 63, 96]. Conversely, another picture used in some papers [65, 67, 93, 97] consists in assuming that for pump photon excitation energies above that of the singlet level, triplets may be formed not only by ISC but also through exciton fission, fusion, recombination of photogenerated polarons or any mixture of phenomena which is then described empirically by a *constant yield of triplet formation* ϕ_T instead of a constant ISC rate. Each absorbed photon will produce a triplet state with a probability ϕ_T and a singlet state with a probability $1 - \phi_T$. The equations are as follows:

$$\begin{cases} \frac{dS_1}{dt} = \sigma_{abs} I_p (1 - \phi_T) S_0 - \left(\frac{1}{\tau_F} + \sigma_{em} I \right) S_1 \\ \frac{dS_0}{dt} = -\sigma_{abs} I_p S_0 + \left(\frac{1}{\tau_F} + \sigma_{em} I \right) S_1 + \frac{T_1}{\tau_T} \\ \frac{dT_1}{dt} = \sigma_{abs} I_p \phi_T S_0 - \frac{T_1}{\tau_T} \end{cases}$$

The differences in the models appear in Fig. 2.21.

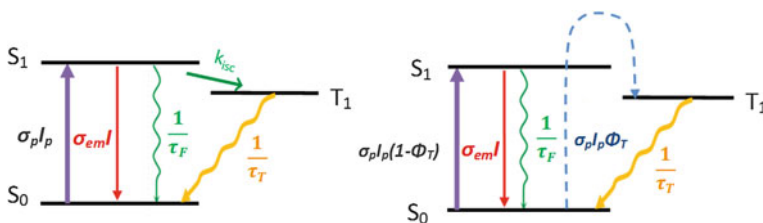


Fig. 2.21 Illustration of the “constant intersystem crossing rate” picture (*left*) versus the “constant triplet yield” picture (*right*) used to describe how triplets are formed in organic pi-conjugated systems under optical excitation

Although there is actually not so much difference in using either one or another model as soon as stimulated emission is absent, the models strongly differ in the presence of stimulated emission, this is why a discussion on these two models is especially relevant when dealing with organic lasers, and may not be that important in other contexts. Indeed, when $I = 0$ the two sets of equations are equivalent upon writing:

$$\phi_T = \frac{k_{ISC}\tau_F}{1 + k_{ISC}\tau_F}$$

In general, the intersystem crossing time constant $1/k_{ISC} \sim 10^{-7}$ s is much longer than the fluorescence lifetime $\tau_F \sim 10^{-9}$ s, so that the triplet yield is simply $\phi_T \approx k_{ISC}\tau_F$ (~ 1 %).

Solving the above rate equations in the steady-state is straightforward (all derivatives are set to zero) and enables picking up the main physical difference between the two models: in the “constant triplet yield” approach, the steady-state triplet population T_1 increases both with the pump intensity and with the laser intensity I ; on the contrary in the “constant rate” approach, ISC is one of the channels which can be activated to deplete the singlet state (with fluorescence, IC, SE...): this means that if stimulated emission becomes strong enough ($I > I_{sat}$) then the feeding rate of the triplet level vanishes and T_1 hence decreases when the laser intensity I increases, for a fixed pump intensity.

2.6 Temporal Dynamics of Organic Solid State Lasers

Recent reports have shown the termination of lasing after a few ns [62] in polymer guest/host systems (see also Fig. 2.23) or a few tens of ns [67] in small-molecular lasers after pump turn-on in case of long-pulse pumping: these aspects are also essential in the context of electrical pumping. The great majority of optically pumped solid-state laser are operating with fs to ns pulse duration, limiting the effect of triplet states.

In this section, we derive a simple design formula for the pulsewidth and a condition for CW lasing, and we present afterwards the results of a numerical simulation from the above-exposed equations in a simple case.

2.6.1 The CW Lasing Condition

True CW lasing in organic solid-state lasers (that is, without rotating the medium to mimic the flow of a liquid dye laser, for instance) is a long-thought objective that has not been achieved yet at the time of writing this book [63].

In order to derive a simple useful analytical CW lasing condition, we first consider the previous rate equations within the framework of the “constant rate” model, and solve them at steady state ($d/dt = 0$). The equation for the triplet state reads

$$T_1^{ss} = k_{ISC}\tau_T S_1^{ss}$$

where T_1^{ss} and S_1^{ss} are the steady-state population of the T_1 and S_1 state, respectively. In order to have a rough estimate, we can assume that the only cause of loss in the system is Triplet Absorption. We neglect STA for instance, and we don't take into account other losses in the cavity. CW lasing will then be possible whenever triplet absorption probability will be lower than stimulated emission probability, or

$$\sigma_{TT}T_1^{ss} < \sigma_{em}S_1^{ss}$$

or

$$\sigma_{TT}k_{ISC}\tau_T < \sigma_{em}$$

simplified condition for CW lasing in an organic laser

It is clear from the typical orders of magnitude exposed in Table 2.1 that this condition is *not met* in most organic systems (σ_{em} and σ_{TT} have roughly the same order of magnitude but k_{ISC} is much higher than $1/\tau_T$, the triplet state is filled much more rapidly than it is depleted).

A good material for CW lasing should then have a low triplet absorption cross-section, a low ISC rate and a small triplet lifetime to allow the triplet population to pour out quickly. Furthermore the triplet absorption spectrum should be shifted as much as possible away from the emission spectrum to enable the previous relation to hold at a given wavelength within the emission spectrum, relaxing the very hard condition on ISC rate and triplet lifetime.

If we look for the CW lasing condition with the *constant yield* approach, we may assume that pumping occurs at a constant rate $G = \sigma_{abs}I_p S_0$ (no ground state depletion), and without any assumption on compared dynamics of triplets versus singlets, the condition $\sigma_{TT}T_1^{ss} < \sigma_{em}S_1^{ss}$ translates into a relation where the CW laser intensity I_{CW} intervenes:

$$\frac{\sigma_{em}\tau_F}{\sigma_{TT}\tau_T} \left(\frac{1 - \phi_T}{\phi_T} \right) > 1 + \frac{I_{CW}}{I_{sat}}$$

With $I_{sat} = \frac{1}{\sigma_{em}\tau_F}$. Not surprisingly this relation is identical to the “constant rate” formulation $\sigma_{TT}k_{ISC}\tau_T < \sigma_{em}$ when $I_{CW} = 0$, which is the limit where the constant rate and constant yield models merge. The condition on σ_{TT} appears to be harder to meet when I_{CW} becomes comparable or higher than I_{sat} : this is physically because if the intracavity intensity is high, the singlet state is depleted, which is not the case of the triplet state, as the latter is continuously filled by the pump at a constant rate $\phi_T\sigma_{abs}I_p S_0$ whatever the laser intensity.

Comparing these models for CW laser action remains highly speculative; it is however useful to have in mind the simple rule-of-thumb given by the constant ISC model which is an adequate and simple rule to work with.

Recently, Zhang and Forrest [63] have published a theoretical paper predicting that in some optically pumped organic semiconductor lasers based on guest/host systems, two threshold pump intensities exist; one for pulsed lasing, I_{PS} , and another for continuous-wave (CW) lasing, I_{CW} . The theory presented in this paper predicts a decrease in I_{CW} from 32 kW/cm², or well above the damage threshold, to 2.2 kW/cm², for a laser employing 4-(dicyanomethylene)-2-methyl-6-julolidyl-9-enyl-4H-pyran-doped tris(8-hydroxyquinoline) aluminum if the triplets can be effectively removed from the emissive guest. They hence show that the lasing duration can be extended to nearly 100 μ s, ultimately limited by degradation of the lasing medium when a “triplet manager” molecule, 9,10-di(naphtha-2-yl)anthracene, is blended into the gain region of an otherwise conventional distributed feedback OSL. The triplet manager facilitates radiative singlet transfer while suppressing nonradiative triplet transfer to the emitter molecule, thus reducing the triplet-induced losses.

2.6.2 Maximum Pulsewidth for Organic Lasers

The consequence of the absence of observed CW lasing action in organic solid-state lasers is the existence of a finite, maximum pulse width under CW pumping, which was initially observed under flashlamp pumping with μ s pump pulses [16].

We assume that triplets are formed through ISC (we use here a constant rate model), at a rate which is much slower than the time needed to reach a steady-state singlet population S_1^{ss} . The dynamics of the singlet states (controlled by a time constant $\sim \tau_F$) is thus supposed to be much faster than the triplet dynamics. Here we also assume that triplet absorption (T–T) results in a loss of laser photons, but not in an appreciable loss of triplet population (see Sect. 2.3.4: it was shown by Yang et al. [74] that 80 % of the high-lying T_n states created by TT absorption in F8BT fall back to the T_1 state within 300 fs). With these simplifying assumptions, the triplet population follows:

$$\frac{dT_1}{dt} = k_{ISC}S_1^{ss} - \frac{T_1}{\tau_T}$$

T_1 hence increases in a monoexponential way:

$$T_1(t) = k_{ISC}\tau_T S_1^{ss} \left[1 - e^{-\frac{t}{\tau_T}} \right]$$

until the triplet state population reaches the steady-state value $T_1^{ss} = k_{ISC}\tau_T S_1^{ss}$.

In the case where the CW lasing condition presented above $\sigma_{TT}T_1^{ss} > \sigma_{em}S_1^{ss}$ is not met, then lasing terminates at time t_L given by $t_L = -\tau_T \ln\left(1 - \frac{\sigma_{em}}{\sigma_{TT}k_{ISC}\tau_T}\right)$; if t_L is significantly smaller than the triplet lifetime, then this expression becomes:

$$t_L \sim \frac{\sigma_{em}}{\sigma_{TT}k_{ISC}}$$

typical maximum pulse length of an organic laser

As in addition σ_{em} and σ_{TT} have the same order of magnitude, an easy rule-of-thumb is

$$t_L \sim 1/k_{ISC}$$

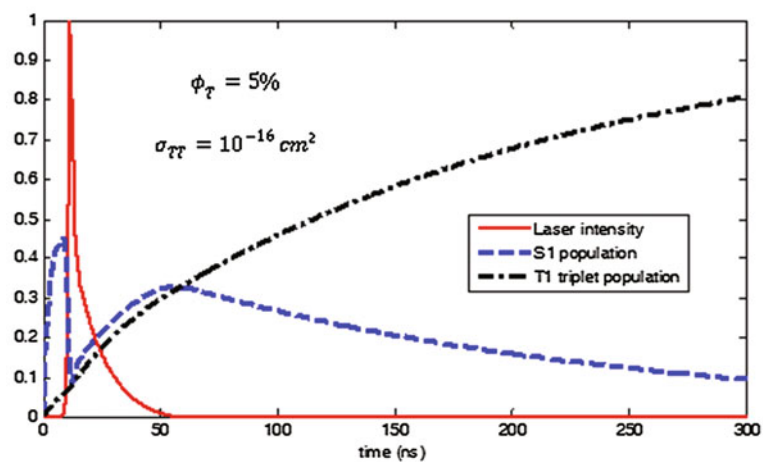
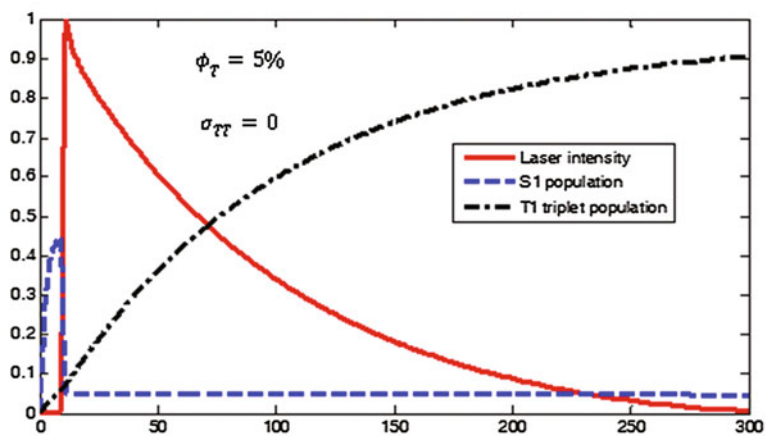
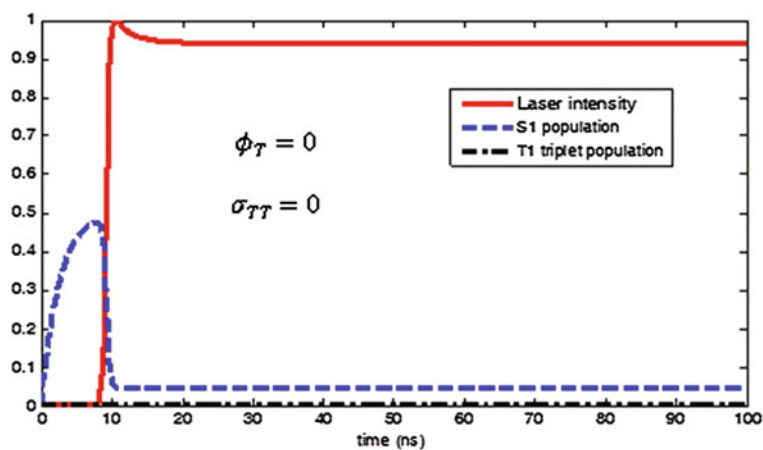
The pulsewidth is expected to vary from a few ns to a few μ s depending essentially on the ISC rate, and has a typical value of ~ 100 ns.

2.6.3 Temporal Dynamics Simulations

We can go further and solve the coupled rate equations and photon density equation. Here the constant yield approach is used. However numerical simulations revealed only little difference between the two (as discussed earlier, there might be a difference essentially in the saturated regime).

Simulations are shown in Fig. 2.22. The first simulation (1) represents the case of a pure 4-level system, that is $\Phi_T = 0$ (and $\sigma_{TT} = 0$ even though this value does not intervene in the simulation as the triplet state is not populated): the startup behavior is clearly seen here because we choose here a cavity much longer than the active medium, meaning that a photon spends most of its time in air between the two mirrors than in the polymer film, which causes quite a long oscillation buildup time (see Chap. 4 for more details about the so-called VEC SOL laser architecture). During this time the singlet density rises to a high value before laser oscillation starts; when the laser intensity reaches the laser saturation intensity I_{sat} (here $I = I_{sat}$ is reached at $t = 8.5$ ns), the singlet state is rapidly depopulated until it clamps to its steady-state value (here 0.05). The laser enters a CW stable regime from $t \sim 20$ ns in this particular case.

The simulation (2) has exactly the same parameters except that some triplet filling is added with a fixed quantum yield $\phi_T = 5\%$, but triplets are assumed to be non absorbing, i.e. σ_{TT} is fixed to 0. This is equivalent (only at $I = 0$ as discussed earlier) to an intersystem crossing rate fixed around 10^7 s^{-1} and a triplet state lifetime of $100 \mu\text{s}$, with a radiative singlet lifetime of 5 ns , which are all very typical values. Interestingly, we notice that the triplet population grows up until it quickly becomes the dominant population in the system, meaning that the ground state S_0 is depopulated in favor of the triplet state. Because the pumping intensity is supposed to be constant, the pumping rate (which is proportional to S_0)



◀ **Fig. 2.22** Results of the simulations showing the evolution of the singlet density S_1 (= number of molecules in the S_1 state/total number of molecules), the triplet density T_1 and the normalized laser intensity I versus time in an organic laser pumped with a constant intensity I_p . The specific structure considered here is a VECSEL-type organic laser (see Chap. 4), which allows visualizing the turn-on dynamics with a comparable timescale. The following parameters are taken for the simulation: thickness of the active medium = 10 μm , absorption = 80 %, absorption cross section = $10\text{--}16\text{ cm}^2$; cavity length = 20 mm; outcoupling = 2 % (the reflectivity of the cavity mirrors are respectively taken to 1 and 0.98), passive losses = 2 % per single pass in the gain medium; fluorescence lifetime = 5 ns; emission cross section = $10\text{--}16\text{ cm}^2$; molecular density $N = 1019\text{ cm}^{-3}$. The pump intensity is fixed to the pump saturation intensity $I_p = I_{p,\text{sat}} = \frac{hc}{\lambda_p \sigma_{\text{abs}} \tau} = 0.5\text{ MW/cm}^2$, that is 20 times above the steady-state threshold Case 1 (*top*): triplet yield and triplet absorption cross sections are fixed to 0 (4-level case); case 2 (*middle*): a fixed triplet yield of 5 % is supposed, but triplets do not absorb laser light; case 3 (*bottom*): a fixed triplet yield of 5 % is considered together with a triplet absorption cross section of 10^{-16} cm^2

decreases, which would tend to decrease the S_1 density. Actually the S_1 density is just reduced below the clamping value which ensures that gain = losses, meaning that the intensity will start to decrease. When this happens, the downward stimulated emission rate from S_1 to S_0 decreases also which tends to stabilize the S_1 density irrespective of a diminution of the pumping rate. This crude model is informative in a sense that even with non-absorbing triplet species or in absence of any triplet quenching phenomenon added to the model, we have a limitation in the pulse duration linked only to the depopulation of the ground state toward the triplet state. Here the laser pulse stops completely after 300 ns.

The simulation (3) at last shows the same system with the same parameters except that some Triplet absorption (TA) is added through a triplet excited state absorption $\sigma_{TT} = 10^{-16}\text{ cm}^2$. As expected in this case, the emitted pulse is still shorter, here it stops after 50 ns (but is less than 10 ns FWHM). The singlet density increases when the laser intensity drops significantly, which can be interpreted as a kind of Q-switching provided by the triplet losses. Note however that by using equations above we ignored triplet state depletion by absorption of laser light: although this is certainly true to consider that once in a highly-excited state T_n , the molecules may undergo a rapid internal conversion back to the T_1 state, they may also be removed to dissociative states or undergo internal conversion back to singlet states, among other possibilities. If we suppose that all laser photons absorbed from a T_1 state represent a net loss for the triplet population, then the curves obtained in cases (2) and (3) of Fig. 2.22 would be very similar, meaning that TA would play only a minor role in the CW impediment of organic lasers in such a case.

Recently, the compared influence of Triplet Absorption (TA) versus Triplet-Singlet annihilation (TSA) in the limited pulse width obtainable from an organic laser has become a subject under debate. Giebink and Forrest [67] studied laser dynamics in a DFB laser and related the experiments to TSA only; Lehnhardt [62] showed in a polymer laser made of MEH-PPV with F8BT that TSA and TA were both important, TA becoming notably predominant at high excitation densities.

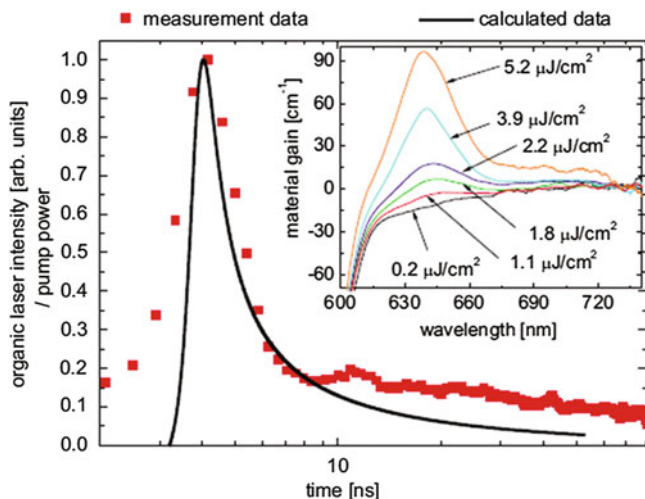


Fig. 2.23 Illustration of the finite pulsewidth obtainable from an organic Solid-state laser. Here the F8BT/MEHPPV laser is pumped by a laser diode with a pulse length of 70 ns; lasing terminates at ~ 10 ns only. Courtesy of T. Riedl. Reprinted with permission from [62]. Copyright (2010) by the American Physical Society

In such a case, the experimental pulse duration from the laser is only ~ 3 ns, as shown in Fig. 2.23.

2.6.4 Is It Better to Characterize Organic Lasers with Fluence (J/cm^2) or Intensity (W/cm^2)?

As organic lasers only emit pulses of light, one may wonder what is the most relevant parameter to measure in a working laser for both the pump and the output beam: is it an energy per pulse (or a related fluence in J/cm^2) or an intensity per pulse (or, in exact radiometric terms, an irradiance) in W/cm^2 ? In many literature reports, both are used evenly, and this deserves some particular attention.

For someone using the laser, the unit will primarily depend on the targeted application. For nonlinear optics for instance, only the peak power (and hence the intensity) is important, while for bio-applications where a certain amount of light energy is needed to treat a tissue or accumulate data, no matter the time, and of course the energy is more valuable.

However, when characterizing a laser, as stimulated processes (absorption and emission) depend on intensities, it is generally not very relevant to draw physical argumentations based on energies. Let's discuss it in more detail. If we consider a medium pumped by a constant pump intensity I_p from $t > 0$, then the singlet state population will "load", firstly without SE as far as the threshold is not reached yet,

with an “effective” time constant given by $\tau_{\text{eff}} = \frac{\tau}{1 + \sigma_{\text{abs}} \tau I_p}$ (obtained from the rate equations with $I = 0$). The effective loading time can be significantly lower than the radiative lifetime if the pump intensity is higher than the *pump* saturation intensity $1/\sigma_{\text{abs}} \tau$ (in photonic units).

If the pump pulse $T_p \ll \tau_{\text{eff}}$, then the pump can be seen as a Dirac pulse; in this case, as far as some molecules have been promoted to the S_1 level, they can only emit a laser photon (or a fluorescence photon, or lose their energy by any means), just *once* for one given pump pulse. In this case it is relevant to measure the energy per pulse. The laser is an “energy storing” device, it stores the energy pump during at most a time equal to the radiative lifetime, and delivers part of this stored energy in a single laser pulse.

If $T_p > \tau_{\text{eff}}$ then a given emitter can undergo several cycles of absorption/emission during one single pulse. Then even though a steady state may not be reached within one pulse, the situation is more like a CW laser working intermittently, or an “energy-converting” device which continuously converts the pump light into laser light. In cases where it is easy to measure the output power of the laser, one can compare the number of emitted photons during a pulse to the number of emitters in the active region to count how many times a given emitter has been used during the pulse [98]. In such a case, intensity is the only relevant parameter.

In particular, if one wants to compare the thresholds or the efficiencies of two different lasers, comparing the fluences (in J/cm^2) has no meaning if the pump pulse durations are not identical and both higher than the effective lifetime (e.g. 1 vs. 10 ns), but it will not be problematic to compare the energies with a fs-pump laser and with a ps-pump laser as for the organic medium, these two pump sources are equally seen as ultrashort “Dirac” pulses providing a given amount of energy.

References

1. W. Holzer et al., Spectroscopic and travelling-wave lasing characterisation of Gilch-type and Horner-type MEH-PPV. *Synth. Met.* **140**(2–3), 155–170 (2004)
2. J.C. Ribierre et al., Amplified spontaneous emission and lasing properties of bisfluorene-cored dendrimers. *Appl. Phys. Lett.* **91**(081108) (2007)
3. E. Ishow et al., Multicolor emission of small molecule-based amorphous thin films and nanoparticles with a single excitation wavelength. *Chem. Mater.* **20**(21), 6597–6599 (2008)
4. C.H. Kim et al., Modeling the low-voltage regime of organic diodes: origin of the ideality factor. *J. Appl. Phys.* **110**(9), 093722 (2011)
5. V. Coropceanu et al., Hole- and electron-vibrational couplings in Oligoacene crystals: intramolecular contributions. *Phys. Rev. Lett.* **89**(27), 275503 (2002)
6. M. Malagoli, J.L. Bredas, Density functional theory study of the geometric structure and energetics of triphenylamine-based hole-transporting molecules. *Chem. Phys. Lett.* **327**(1–2), 13–17 (2000)
7. V. Coropceanu et al., Charge transport in organic semiconductors. *Chem. Rev.* **107**(4), 926 (2007)

8. Y. Shirota, H. Kageyama, Charge carrier transporting molecular materials and their applications in devices. *Chem. Rev.* **107**(4), 953 (2007)
9. A. Moliton, *Optoelectronics of molecules and polymers* (Springer, New York, 2005)
10. P.M. Borsenberger, L. Pautmeier, H. Bassler, Charge transport in disordered molecular solids. *J. Chem. Phys.* **94**(8), 5447–5454 (1991)
11. I.I. Fishchuk et al., Nondispersive polaron transport in disordered organic solids. *Phys. Rev. B* **67**(22), 224303 (2003)
12. L. Li, H. Kosina, Charge transport in organic semiconductor devices, in *Organic Electronics*, ed. by T. Grasser, G. Meller (Springer, Berlin, 2010), p. 301
13. S. Moller, G. Weiser, C. Lapersonne-Meyer, Excitonic photoconductivity of 4BCMU polydiacetylene single crystals. *Synth. Met.* **116**(1–3), 23–26 (2001)
14. S.F. Alvarado et al., Direct determination of the exciton binding energy of conjugated polymers using a scanning tunneling microscope. *Phys. Rev. Lett.* **81**(5), 1082–1085 (1998)
15. P.P. Sorokin, R. Lankard, Stimulated emission observed from an organic dye, chloro-aluminium phthalocyanine. *IBM J. Res. Develop* **10**, 162–163 (1966)
16. F.P. Schafer (ed.), *Dye Lasers*. Topics in Applied Physics, vol. 3, ed. by F.P. Schafer (Springer, Berlin, 1973), p. 285
17. R. Bornemann, U. Lemmer, E. Thiel, Continuous-wave solid-state dye laser. *Opt. Lett.* **31**(11), 1669 (2006)
18. S. Chénais, S. Forget, Recent advances in solid-state organic lasers. *Polym. Int.* **61**(3), 390–406 (2012)
19. C.H.J. Wells, Introduction to Molecular Photochemistry. Chapman and Hall Chemistry Textbook Series (Chapman and Hall, New York, 1972)
20. J.M. Holt, *Ultrafast Optical Measurements of Charge Generation and Transfer Mechanisms of Pi-conjugated Polymers for Solar Cell Applications*, University of Utah, 2009
21. P. Chaquin, F. Fuster, Orbimol Laboratoire de Chimie Théorique, (UPMC Univ Paris 6, UMR CNRS 7616, Paris, 2012), <http://www.lct.jussieu.fr/pagesperso/orbimol/>
22. H.A.M. van Mullekom et al., Developments in the chemistry and band gap engineering of donor-acceptor substituted conjugated polymers. *Mater. Sci. Eng. R Reports* **32**(1), 1–40 (2001)
23. J. Roncali, Molecular engineering of the band gap of π -conjugated systems: facing technological applications. *Macromol. Rapid Commun.* **28**(17), 1761–1775 (2007)
24. C.A. Coulson, Excited electronic levels in conjugated molecules: I. Long wavelength ultra-violet absorption of naphthalene, anthracene and homologs. *Proc. Phys. Soc.* **60**(3), 257 (1948)
25. T.H. Fay, S.D. Graham, Coupled spring equations. *Int. J. Math. Educ. Sci. Technol.* **34**(1), 65–79 (2003)
26. A.C. Tropper et al., Vertical-external-cavity semiconductor lasers. *J. Phys. D Appl. Phys.* **37**(9), R75 (2004)
27. S. Jasprit, *Electronic and Optoelectronic Properties of Semiconductor Structures* (Cambridge University Press, Cambridge, 2007), p. 560
28. G.G. Malliaras et al., Nondispersive electron transport in Alq[₃]. *Appl. Phys. Lett.* **79**(16), 2582 (2001)
29. T. Susdorf et al., Photophysical characterisation of some dipyrromethene dyes in ethyl acetate and covalently bound to poly(methyl methacrylate). *Chem. Phys.* **312**(1–3), 151–158 (2005)
30. I. Gozhyk et al., Polarization properties of solid-state organic lasers. *Phys. Rev. A* **86**(4), 043817 (2012)
31. I. Gozhyk et al., Towards polarization controlled organic micro-lasers. in *Photonics West* (SPIE, San Francisco, 2012)
32. B. Valeur, *Molecular Fluorescence* (Wiley-VCH, Weinheim, 2001)
33. H.-W. Lin et al., Tuning stimulated emission of organic thin films by molecular reorientation. *Appl. Phys. Lett.* **87**(7), 071910–071913 (2005)
34. F.J. Duarte, *Tunable Laser Applications*, 2nd edn. (CRC Press, New York, 2009)

35. M. Goossens et al., Subpicosecond pulses from a gain-switched polymer distributed feedback laser. *Appl. Phys. Lett.* **85**(1), 31 (2004)
36. P. Atkins, J.D. Paula, *Physical Chemistry* (Oxford University Press, New York, 2006)
37. M. Fox, *Optical Properties of Solids*. (Oxford Master Series in Condensed Matter Physics) (Oxford University Press, New York, 2002)
38. S. Forget et al., Red-emitting fluorescent organic light emitting diodes with low sensitivity to self-quenching. *J. Appl. Phys.* **108**(064509) (2010)
39. S.J. Strickler, R.A. Berg, Relationship between absorption intensity and fluorescence lifetime of molecules. *J. Chem. Phys.* **37**(4), 814–822 (1962)
40. W. Holzer, A. Penzkofer, T. Tsuboi, Absorption and emission spectroscopic characterization of Ir(ppy)₃. *Chem. Phys.* **308**(1–2), 93–102 (2005)
41. M. Reufer, J.M. Lupton, U. Scherf, Stimulated emission depletion of triplet excitons in a phosphorescent organic laser. *Appl. Phys. Lett.* **89**(14), 141111–141113 (2006)
42. S.W. Hell, J. Wichmann, Breaking the diffraction resolution limit by stimulated emission: stimulated-emission-depletion fluorescence microscopy. *Opt. Lett.* **19**(11), 780–782 (1994)
43. M.D. McGehee et al., Semiconducting polymer distributed feedback lasers. *Appl. Phys. Lett.* **72**(13), 1536–1538 (1998)
44. S. Chandra et al., Tunable ultraviolet laser source based on solid-state dye laser technology and CsLiB₆O₁₀ harmonic generation. *Opt. Lett.* **22**(4), 209 (1997)
45. S. Forget et al., Tunable ultraviolet vertically-emitting organic laser. *Appl. Phys. Lett.* **98**(13), 131102 (2011)
46. X.H. Yang et al., Highly efficient polymeric electrophosphorescent diodes. *Adv. Mater.* **18**(7), 948 (2006)
47. Y.F. Pedash et al., Spin-orbit coupling and luminescence characteristics of conjugated organic molecules. I. Polyacenes. *J. Mol. Struct. (Theochem)* **585**(1), 49–59 (2002)
48. R.F. Kubin, A.N. Fletcher, The effect of oxygen on the fluorescence quantum yields of some coumarin dyes in ethanol. *Chem. Phys. Lett.* **99**(1), 49–52 (1983)
49. G. Tsiminis et al., A two-photon pumped polyfluorene laser. *Appl. Phys. Lett.* **94**(25), 253304 (2009)
50. Y. Mo et al., Ultraviolet-emitting conjugated polymer poly(9,9[prime or minute]-alkyl-3,6-silafluorene) with a wide band gap of 4.0 eV. *Chem. Commun.* **39**, 4925 (2005)
51. N. Johansson et al., Solid-state amplified spontaneous emission in some spiro-type molecules: a new concept for the design of solid-state lasing molecules. *Adv. Mater.* **10**(14), 1136 (1998)
52. T. Spehr et al., Organic solid-state ultraviolet-laser based on spiro-terphenyl. *Appl. Phys. Lett.* **87**(16), 161103 (2005)
53. J.V. Caspar, T.J. Meyer, Application of the energy gap law to nonradiative, excited-state decay. *J. Phys. Chem.* **87**(6), 952–957 (1983)
54. P. Del Carro et al., Near-infrared imprinted distributed feedback lasers. *Appl. Phys. Lett.* **89**(20), 201105 (2006)
55. S. Yuyama et al., Solid state organic laser emission at 970 nm from dye-doped fluorinated-polyimide planar waveguides. *Appl. Phys. Lett.* **93**(2), 023306 (2008)
56. M. Casalboni et al., 1.3 μ m light amplification in dye-doped hybrid sol-gel channel waveguides. *Appl. Phys. Lett.* **83**(3), 416 (2003)
57. C. Winder, N.S. Sariciftci, Low bandgap polymers for photon harvesting in bulk heterojunction solar cells. *J. Mater. Chem.* **14**(7), 1077–1086 (2004)
58. R.E. Peierls, *Quantum Theory of Solids* (Oxford University Press, London, 1956)
59. H. Föll, http://www.tf.uni-kiel.de/matwis/amat/semi_en/kap_a/advanced/ta_4_1.html
60. S.A. Jenekhe, A class of narrow-band-gap semiconducting polymers. *Nature* **322**(6077), 345–347 (1986)
61. M.A. Baldo et al., Highly efficient phosphorescent emission from organic electroluminescent devices. *Nature* **395**(6698), 151–154 (1998)

62. M. Lehnhardt et al., Impact of triplet absorption and triplet-singlet annihilation on the dynamics of optically pumped organic solid-state lasers. *Phys. Rev. B* **81**(16), 165206 (2010)
63. Y. Zhang, S.R. Forrest, Existence of continuous-wave threshold for organic semiconductor lasers. *Phys. Rev. B* **84**(24), 241301 (2011)
64. S. Schols et al., Triplet excitation scavenging in films of conjugated polymers. *Chem. Phys. Chem.* **10**(7), 1071–1076 (2009)
65. S. Kéna-Cohen et al., Plasmonic sinks for the selective removal of long-lived states. *ACS Nano* **5**(12), 9958–9965 (2011)
66. M.A. Baldo, R.J. Holmes, S.R. Forrest, Prospects for electrically pumped organic lasers. *Phys. Rev. B* **66**(3), 035321 (2002)
67. N.C. Giebink, S.R. Forrest, Temporal response of optically pumped organic semiconductor lasers and its implication for reaching threshold under electrical excitation. *Phys. Rev. B* **79**(073302) (2009)
68. N.C. Giebink, Y. Sun, S.R. Forrest, Transient analysis of triplet exciton dynamics in amorphous organic semiconductor thin films. *Org. Electron.* **7**(5), 375–386 (2006)
69. A. Kohler, H. Bassler, Triplet states in organic semiconductors. *Mater. Sci. Eng. R Reports* **66**(4–6), 71–109 (2009)
70. S.P. McGlynn, T. Azumi, M. Kinoshita, *Molecular Spectroscopy of the Triplet State*, ed.(P.-H. International, Hemel Hempstead, 1969). ISBN: 0135996627
71. A. Köhler, D. Beljonne, The singlet–triplet exchange energy in conjugated polymers. *Adv. Funct. Mater.* **14**(1), 11–18 (2004)
72. J. Michl, E.W. Thulstrup, Why is azulene blue and anthracene white? A simple mo picture. *Tetrahedron* **32**(2), 205–209 (1976)
73. C. Cohen-Tannoudji, B. Diu, F. Laloe, *Quantum mechanics/Claude Cohen-Tannoudji, Bernard Diu, Franck Laloe; translated from the French by Susan Reid Hemley, Nicole Ostrowsky, Dan Ostrowsky* (Wiley, New York, 1977)
74. X. Yang et al., Saturation, relaxation, and dissociation of excited triplet excitons in conjugated polymers. *Adv. Mater.* **21**(8), 916–919 (2009)
75. C. Adachi et al., Nearly 100% internal phosphorescence efficiency in an organic light-emitting device. *J. Appl. Phys.* **90**(10), 5048–5051 (2001)
76. S. Schols, *Device Architecture and Materials for Organic Light-Emitting Devices*, 1st edn. (Springer, Berlin, 2011). ISBN: 9789400716070
77. J. Lakowicz, *Principles of Fluorescence Spectroscopy*, 3rd edn. (Springer, New York, 2006)
78. R.M. Clegg, Förster resonance energy transfer—FRET what is it, why do it, and how it's done, in *Laboratory Techniques in Biochemistry and Molecular Biology*, vol. 33, ed. by T.W.J. Gadella, (Elsevier, Amsterdam, 2009), pp. 1–57
79. D.F. Evans, 257. Perturbation of singlet-triplet transitions of aromatic molecules by oxygen under pressure. *J. Chem. Soc. (Resumed)*, **1957**, 1351–1357 (1957)
80. M. Lebental et al., Diffusion of triplet excitons in an operational organic light-emitting diode. *Phys. Rev. B* **79**(165318) (2009)
81. R.R. Lunt, et al., Exciton diffusion lengths of organic semiconductor thin films measured by spectrally resolved photoluminescence quenching. *J. Appl. Phys.* **105**(053711) (2009)
82. G. Weber, Dependence of the polarization of the fluorescence on the concentration. *Trans. Faraday Soc.* **50**, 552–555 (1954)
83. S.Y. Arzhantsev et al., On the singlet–singlet annihilation of the excited states of Rhodamine 3B in a polymer film. *Laser Phys.* **9**(2), 466–469 (1999)
84. C. Gärtner, *Organic Laser Diodes: Modelling and Simulation* (Universitätsverlag Karlsruhe, Karlsruhe, 2009)
85. M.A. Baldo et al., Excitonic singlet-triplet ratio in a semiconducting organic thin film. *Phys. Rev. B* **60**(20), 14422–14428 (1999)
86. E.J.W. List et al., Direct evidence for singlet-triplet exciton annihilation in Ir^{III} -conjugated polymers. *Phys. Rev. B* **66**(23), 235203 (2002)

87. M.A. Baldo, C. Adachi, S.R. Forrest, Transient analysis of organic electrophosphorescence. II. Transient analysis of triplet–triplet annihilation. *Phys. Rev. B.* **62**(16), 10967–10977 (2000)
88. A. Siegman, *Lasers* (University Science Books, Mill Valey, 1986)
89. M. Koschorreck et al., Dynamics of a high-Q vertical-cavity organic laser. *Appl. Phys. Lett.* **87**(181108) (2005)
90. L.A. Coldren, S.W. Corzine, *Diode Lasers and Photonic Integrated Circuits* (Wiley-VCH, New York, 1997)
91. C. Delsart, *Lasers & Optique Non Linéaire* (Ellipses, Paris, 2008), p. 426
92. C. Gartner et al., The influence of annihilation processes on the threshold current density of organic laser diodes. *J. Appl. Phys.* **101**(2), 023107 (2007)
93. G. Lanzani et al., Triplet-exciton generation mechanism in a new soluble (Red-Phase) Polydiacetylene. *Phys. Rev. Lett.* **87**(18), 187402 (2001)
94. J. Widengren, R. Rigler, Ü. Mets, Triplet-state monitoring by fluorescence correlation spectroscopy. *J. Fluoresc.* **4**(3), 255–258 (1994)
95. A. Penzkofer, W. Falkenstein, Theoretical investigation of amplified spontaneous emission with picosecond light pulses in dye solutions. *Opt. Quant. Electron.* **10**(5), 399–423 (1978)
96. C. Gartner et al., The influence of annihilation processes on the threshold current density of organic laser diodes. *J. Appl. Phys.* **101**(2), 023107–023109 (2007)
97. C. Zenz et al., Ultrafast photogeneration mechanisms of triplet states in para-hexaphenyl. *Phys. Rev. B* **59**(22), 14336–14341 (1999)
98. H. Rabbani-Haghighi et al., Highly efficient, diffraction-limited laser emission from a vertical external-cavity surface-emitting organic laser. *Opt. Lett.* **35**(12), 1968–1970 (2010)
99. D. Cahen, A. Kahn, E. Umbach, Energetics of molecular interfaces. *Mater. Today* **8**(7), 32–41 (2005)
100. H.A.M. van Mullekom et al., Developments in the chemistry and band gap engineering of donor-acceptor substituted conjugated polymers. *Mater. Sci. Eng. R Reports* **32**(1), 1 (2001)
101. M.P. Lettinga, H. Zuilhof, M.A.M.J. van Zandvoort, Phosphorescence and fluorescence characterization of fluorescein derivatives immobilized in various polymer matrices. *Phys. Chem. Chem. Phys.* **2**(16), 3697–3707 (2000)
102. T.G. Pavlopoulos et al., Laser action from syn-(methyl, methyl) biman. *J. Appl. Phys.* **60**(11), 4028–4030 (1986)
103. A. Costela et al., Polymeric matrices for lasing dyes: recent developments. *Laser Chem.* **18**(1–2), 63–84 (1998)
104. J. Yu et al., Singlet-triplet and triplet–triplet interactions in conjugated polymer single molecules. *J. Phys. Chem. B* **109**(20), 10025–10034 (2005)
105. M.A. Stevens et al., Exciton dissociation mechanisms in the polymeric semiconductors poly(9,9-dioctylfluorene) and poly(9,9-dioctylfluorene-co-benzothiadiazole). *Phys. Rev. B* **63**(16), 165213 (2001)
106. E.J.W. List et al., Direct evidence for singlet-triplet exciton annihilation in pi-conjugated polymers. *Phys. Rev. B* **66**(235203) (2002)
107. G.D. Hale, S.J. Oldenburg, N.J. Halas, Observation of triplet exciton dynamics in conjugated polymer films using two-photon photoelectron spectroscopy. *Phys. Rev. B* **55**(24), R16069–R16071 (1997)
108. D. Hertel, K. Meerholz, Triplet-polaron quenching in conjugated polymers. *J. Phys. Chem. B* **111**(42), 12075–12080 (2007)

Organic Solid-State Lasers

Forget, S.; Chénais, S.

2013, XI, 169 p. 88 illus., 78 illus. in color., Hardcover

ISBN: 978-3-642-36704-5